

Infocommunications Journal

A PUBLICATION OF THE SCIENTIFIC ASSOCIATION FOR INFOCOMMUNICATIONS (HTE)

SEPTEMBER 2018

Volume X

Number 3

ISSN 2061-2079

GUEST EDITORIAL

Featured papers of the H-SPACE 2018 conference *László Bacsaárdi and Kálmán Kovács* 1

PAPERS OF THE SPECIAL ISSUE

Using Radio Wave Satellite Propagation Measurements
for Rain Intensity Estimation *Bernard Adjei-Frimpong and László Csurgai-Horváth* 2

Optical transfer in space communication *Andrea Farkasvölgyi and István Frigyes* 9

Comparing Calculated and Measured Losses in
a Satellite-Earth Quantum Channel..... *Máté Galambos and László Bacsaárdi* 14

PAPERS FROM OPEN CALL

Ontology based Indoor Navigation Service for
the ILONA System *Dániel Péter Kun, Erika Baksáné Varga and Zsolt Tóth* 21

Automatic classification possibilities of the voices
of children with dysphonia *Miklós Gábrriel Tulics and Klára Vicsi* 30

CALL FOR PAPERS / PARTICIPATION

IEEE/IFIP International Workshop on Analytics for Network and Service Management
AnNet 2019, Washington DC, USA – co-located with IEEE IM 2019 37

IEEE International Conference on Smart Technologies
IEEE EUROCON 2019, Novi Sad, Serbia 38

IEEE Global Communications Conference
IEEE GLOBECOM 2019, Big Island, Hawaii, USA 41

ADDITIONAL

Guidelines for our Authors 40

Technically Co-Sponsored by



Editorial Board

Editor-in-Chief: ROLLAND VIDA, Budapest University of Technology and Economics (BME), Hungary
Associate Editor-in-Chief: PÁL VARGA, Budapest University of Technology and Economics (BME), Hungary

- | | |
|---|---|
| ÖZGÜR B. AKAN
Koc University, Istanbul, Turkey | MAJA MATIJASEVIC
University of Zagreb, Croatia |
| JAVIER ARACIL
Universidad Autónoma de Madrid, Spain | VACLAV MATYAS
Masaryk University, Brno, Czech Republic |
| LUIGI ATZORI
University of Cagliari, Italy | OSCAR MAYORA
Create-Net, Trento, Italy |
| LÁSZLÓ BACSÁRDI
University of West Hungary | MIKLÓS MOLNÁR
University of Montpellier, France |
| JÓZSEF BÍRÓ
Budapest University of Technology and Economics, Hungary | SZILVIA NAGY
Széchenyi István University of Győr, Hungary |
| STEFANO BREGNI
Politecnico di Milano, Italy | PÉTER ODRY
VTS Subotica, Serbia |
| VESNA GRNOJEVIĆ-BENGIN
University of Novi Sad, Serbia | JAUELICE DE OLIVEIRA
Drexel University, USA |
| KÁROLY FARKAS
Budapest University of Technology and Economics, Hungary | MICHAL PIORO
Warsaw University of Technology, Poland |
| VIKTORIA FODOR
Royal Technical University, Stockholm | ROBERTO SARACCO
Trento Rise, Italy |
| EROL GELENBE
Imperial College London, UK | GHEORGHE SEBESTYÉN
Technical University Cluj-Napoca, Romania |
| CHRISTIAN GÜTL
Graz University of Technology, Austria | BURKHARD STILLER
University of Zürich, Switzerland |
| ANDRÁS HAJDU
University of Debrecen, Hungary | CSABA A. SZABÓ
Budapest University of Technology and Economics, Hungary |
| LAJOS HANZO
University of Southampton, UK | LÁSZLÓ ZSOLT SZABÓ
Sapientia University, Tirgu Mures, Romania |
| THOMAS HEISTRACHER
Salzburg University of Applied Sciences, Austria | TAMÁS SZIRÁNYI
Institute for Computer Science and Control, Budapest, Hungary |
| JUKKA HUHTAMÄKI
Tampere University of Technology, Finland | JÁNOS SZTRIK
University of Debrecen, Hungary |
| SÁNDOR IMRE
Budapest University of Technology and Economics, Hungary | DAMLA TURGUT
University of Central Florida, USA |
| ANDRZEJ JAJSZCZYK
AGH University of Science and Technology, Krakow, Poland | ESZTER UDVARY
Budapest University of Technology and Economics, Hungary |
| FRANTISEK JAKAB
Technical University Kosice, Slovakia | SCOTT VALCOURT
University of New Hampshire, USA |
| KLIMO MARTIN
University of Zilina, Slovakia | JINSONG WU
Bell Labs Shanghai, China |
| DUSAN KOCUR
Technical University Kosice, Slovakia | KE XIONG
Beijing Jiaotong University, China |
| ANDREY KOUCHERYAVY
St. Petersburg State University of Telecommunications, Russia | GERGELY ZÁRUBA
University of Texas at Arlington, USA |
| LEVENTE KOVÁCS
Óbuda University, Budapest, Hungary | |

Indexing information

Infocommunications Journal is covered by Inspec, Compendex and Scopus.
Infocommunications Journal is also included in the Thomson Reuters – Web of Science™ Core Collection, Emerging Sources Citation Index (ESCI)

Infocommunications Journal

Technically co-sponsored by IEEE Communications Society and IEEE Hungary Section

Supporters

FERENC VÁGUJHELYI – president, National Council for Telecommunications and Information Technology (NHIT)
 GÁBOR MAGYAR – president, Scientific Association for Infocommunications (HTE)

Editorial Office (Subscription and Advertisements):
 Scientific Association for Infocommunications
 H-1051 Budapest, Bajcsy-Zsilinszky str. 12, Room: 502
 Phone: +36 1 353 1027
 E-mail: info@hte.hu • Web: www.hte.hu

Articles can be sent also to the following address:
 Budapest University of Technology and Economics
 Department of Telecommunications and Media Informatics
 Tel.: +36 1 463 1102, Fax: +36 1 463 1763
 E-mail: vida@tmit.bme.hu

Subscription rates for foreign subscribers: 4 issues 10.000 HUF + postage

Publisher: PÉTER NAGY

HU ISSN 2061-2079 • Layout: PLAZMA DS • Printed by: FOM Media

Featured papers of the H-SPACE 2018 conference – Guest Editorial

László Bacsárdi and Kálmán Kovács

In 2018, the annual International Conference on Research, Technology and Education of Space has been held the 4th time. The host was the BME Space Forum operated by the Federated Innovation and Knowledge Centre (EIT) of the Faculty of Electrical Engineering and Informatics at the Budapest University of Technology and Economics (BME) – in cooperation with the Hungarian Astronautical Society (MANT), which is the oldest space association in Hungary. Three selected papers are featured in the current issue of the Infocommunications Journal.

The organization of the H-SPACE conference series started in 2015, at a time of growing opportunities arising from ESA recently granting membership to Hungary and the need for a joint presentation of space activities pursued at BME. The selection of the date of the event pays tribute to the successful deployment to orbit and mission of the first Hungarian satellite, the Masat-1, which has been launched on February 13, 2012. The main topic of this year’s conference was “Space research for society on every scale”. The agenda of the conference addressed scientific, technological and educational issues of space research and space activities.

The Federated Innovation and Knowledge Centre (BME EIT) was created at the Faculty of Electrical Engineering and Informatics of Budapest University of Technology and Economics (BME) in 2009 to stimulate the research and development activity and to assist the exploitation of research achievements at the Faculty. Currently, BME EIT also operates the BME Space Forum which mission is to harmonize and coordinate the activity of departments at BME participating in space activities by a common vision and strategy, to recognize the joint human and technical resources and amazing achievements, to make internal and external knowledge transfer more efficient, and to utilize opportunities lying in synergies granted by joint capabilities and unified representation. The common aim of BME Space Forum members is to become the bridge between academic research and production, service application, and to participate all phases of research/development/innovation and application processes of space activity.

The Hungarian Astronautical Society (MANT in Hungarian) is a civil organization in Hungary that gathers space researchers, users of space technology and everyone who is interested in the interdisciplinary and state-of-the-art uses and research of outer space. The society was established in 1956 in Budapest, and it is the only Hungarian member of the International Astronautical Federation (IAF) since 1959. The aim of MANT is to raise public awareness about space activity and space applications. The society also provides an opportunity for space enthusiasts to meet, exchange ideas and work together. MANT, through its members from various fields of science, organizes conferences, youth forums, summer space camps, issues periodicals, releases media

material and holds lectures about space research and connected scientific fields.

The conference was open for both local and international professionals and provided an opportunity to showcase Hungarian scientific, technological, educational and outreach activities, related to space. Detailed information can be found on its website (space.bme.hu). Due to the generous support of our partners, the conference had no registration fee. We had more than 200 registered participants from 11 countries. During the conference, we had 1 keynote lecture, 3 long talks and 26 technical presentations from which 11 authors have submitted a full paper. Among them we selected three papers for the current issue.

Estimation of Clear Sky Level for Satellite Propagation Measurements deals with a years-long-measurement. The European Space Agency launched a communication satellite called ‘Alphasat’ in 2013, with two experimental beacons to carry out a scientific experiment. The ground station at the institute of the authors receives signal from the satellite to characterize the satellite-Earth propagation channel. The main goal of long-term propagation measurements is to improve the existing attenuation models that are published in the relevant ITU-R recommendations.

Optical transfer in space communication presents the possibilities of free-space optical connection in space communication. It summarizes the advantages and disadvantages of optical transmission in case of Near Earth and Deep Space region as well as discusses the application of multichannel or more precise diversity systems.

Comparing Calculated and Measured Losses in a Satellite-Earth Quantum Channel deals with quantum-based satellite communication. It compares the theoretical predictions for channel loss with measured values of QuESS (Quantum Experiment at Space Scale) experiment which realized the first satellite-Earth quantum channel.



László Bacsárdi received his M.Sc. degree in 2006 in Computer Engineering from the Budapest University of Technology and Economics (BME). He wrote his PhD thesis on the possible connection between space communications and quantum communications at the BME Department of Telecommunications in 2012. He is the Vice President of the Hungarian Astronautical Society (MANT).



Kálmán Kovács has PhD in applications of geographic information systems, MSc in mathematical engineering. He has been working for Budapest University of Technology and Economics (BME) since 1984. He is director of the Federated Innovation and Knowledge Centre of BME (BME EIT) and associate professor of Faculty of Electrical Engineering and Informatics of BME (BME VIK). As a minister, he was supervising the Hungarian space activities as member of the Hungarian Space Board (from 1995 to 2012 its Chairman).

Using Radio Wave Satellite Propagation Measurements for Rain Intensity Estimation

Bernard Adjei-Frimpong and László Csurgai-Horváth

Abstract—The European Space Agency launched a communication satellite called Alphasat in 2013, with two experimental beacons to carry out a scientific experiment by measurement at frequencies of 19.7 GHz and 39.4 GHz respectively. Propagation through the atmosphere at these frequencies is affected by the presence of atmospheric gases and other particles like water vapour, rain and ice drops. Rain attenuation is the most significant parameter which degrades the performance of the links by absorbing and scattering radio waves that can be determined as the measured received signal power's deviation from the nominal, non-attenuated level. Rainfall statistical data are also measured and recorded by the propagation terminals to provide additional information to apply prediction methods that require minutes of integration time rain intensity.

In our institute, at the Department of Broadband Infocommunications and Electromagnetic Theory we have set up a ground station to carry out propagation measurements in the Ka/Q band. The station receives the signal from the satellite to characterize the satellite-Earth propagation channel. The beacon receiver station has been operating since 2014, collecting signal power data, and relevant meteorological data as well. The main goal of long-term propagation measurements is to improve the existing attenuation models that are published in the relevant ITU-R recommendations.

In this paper data processing procedures are discussed and exemplified by their application to one year of measurements. In addition it will be shown how the signal attenuation data can be converted to rain intensity that provides a different method to gain meteorological data over the propagation path.

The attenuation statistics obtained from measured time series are compared with models predictions from the relevant ITU-R standard. Then we evaluated the relationship between rain attenuation and rainfall intensity by extracting the rain intensity information using the measured attenuation on the radio path. The results are compared with the local rain-gauge measurements as well.

Index terms—satellite propagation, attenuation statistics, rain rate

I. INTRODUCTION

One of the major challenges, affecting propagating characteristics on terrestrial and satellite communication links at microwave and millimetre wave frequencies are the significance of rain attenuation of electromagnetic waves. Rain attenuation effect, greatly influences the propagation loss experienced by terrestrial communication links, from the

transmitter to receiver. The attenuation by rain depends on the temperature, distribution size, terminal velocity and shape of the raindrops.

Rain attenuation can be measured quite accurately by means of satellite beacon signals. However, since propagation experiments are carried out only in few places across the world and for a limited number of frequencies and link geometry, their results cannot be directly applied to all sites. For this reason, several attenuation models based on physical facts and using available meteorological data have been developed to provide adequate inputs for system margin calculations in all regions of the world.

The Radiocommunication sector of the International Telecommunication Union (ITU-R) provides these set of models which are largely derived from measured data and uses rain intensity and rain height as the main input parameters [1]. The accurate estimation of the prevision of the rain intensity values at any site are needed for a correct terrestrial and satellite radio links design.

The main goal of long-term propagation measurements is to improve the existing attenuation models that are published in the relevant ITU-R recommendations. In the present paper we will introduce the measurements that are conducted at the Budapest University of Technology and Economics, Department of Broadband Infocommunications and Electromagnetic Theory (BME-HVT), the data processing procedures, comparing them with the relevant ITU-R recommendations, and a method how the attenuation data can be converted to rain intensity. In the first phase data pre-processing is performed and the measured received signal power is converted to attenuation. The reference level (clear sky level) is a critical parameter during this process that can be selected on different bases [2].

The propagation measurements are carried out in Ka- and Q-bands based on the unmodulated beacon signal transmitting from the satellite. Our institution is operating a receiver station where analysis is carried in relation to this research [3].

The organization of this paper is as follows. Section II gives a description of equipment used at the receiver station for measurement and the development of a method to study the radio wave attenuation effects in Ka/Q band. Section III describes the effects of rain attenuation for high frequencies in Ka/Q-band satellite communications links. The method applied to convert the measured received signal level to attenuation are analysed in Section IV. Section V shows how the attenuation data can be converted to rain rate. Finally, we evaluate the results and conclude the paper.

¹ Bernard Adjei-Frimpong and László Csurgai-Horváth are with Budapest University of Technology and Economics, Department of Broadband Infocommunications and Electromagnetic Theory, Hungary. e-mail: {bernard.frimpong, laszlo.csurgai}@hvt.bme.hu

II. RECEIVER STATION SET-UP

Alphasat is an European satellite launched in 2013 with two beacons for wave propagation characterization in the Ka (19.701 GHz) and Q (39.403 GHz) band respectively [5]-[7]. A European-wide experimental network [8]-[9] is serving to utilise as efficient as possible the resources aboard of the satellite. Several receiver stations are installed in different countries as it is described in [10]-[13]. BME-HVT also established a beacon receiver station that is located on top of the department’s building at BME, N47.48° latitudes and E19.06° longitudes at a height of 120 m [3]. Other activities to improve the satellite communication technologies are also conducted in our country, as it was published in [5].

The building blocks of the receiver station are modified terrestrial microwave radio equipment with several hardware and firmware modifications. Both the Ka and the Q-band receivers are based on identical outdoor unit (ODU) construction; the difference is only the frequency of the locally synthesized signals to provide an identical 140 MHz IF frequency. As the orbit of Alphasat is low-inclination geosynchronous a tracking system is also operated in order to eliminate the daily variation of the received signal power. Figure 1 is a display of high performance antennas with tracking system.

The ODU is a double conversion heterodyne receiver with synthesized local signal sources. Its original noise figure has been reduced from 5 dB to 3 dB and in order to generate a stable and jitter-free down-converted intermediate frequency (IF) signal, the oscillator block in the ODU is also changed. The reference oscillator of the synthesizers is now designed to achieve a high stability, low phase noise OCXO with less than ± 1.0 ppb/day stability. The down-converted, filtered (bandwidth=100 kHz) and amplified IF signals are connected with a low attenuation coaxial cable to the indoor unit (IDU) and the calibrated gain of the ODU is 100 dB.



Figure 1. High performance antennas with tracking system

The indoor unit is based on a modified I-Q demodulator that processes the incoming IF signal. The 140 MHz IF signal is under sampled with 80 MHz analog/digital converter unit. The role of the quadrature digital downconverter (QDDC) module is to convert down the sampled signal into baseband quadrature component signals. The baseband signals (I, Q) are decimated (512) and filtered by CIC and FIR filters.

The ODU also contains an internal temperature sensor with 1°C accuracy. This sensor is used for the temperature-compensation of the ODU’s amplifier circuits. During the calibration of the ODU in a thermal-chamber the temperature-dependency of the complete receiver chain was determined. The firmware has a built-in compensation table; therefore, the result is a temperature-independent, high accuracy level measurement. The temperature-compensated values are averaged and fed to a fine gain control unit that ensures the nominal 100 dB ODU gain.

The filtered and decimated signal is processed by an 8192 point FFT where the beacon signal can be detected as the highest amplitude spectral component. The carrier amplitude measurement is performed within 1 second and the final data is forwarded after a logarithmic conversion to the data collecting system. The resolution of the received power is 0.2 dBm. By taking into account the speed of A/D conversion, the decimation and the FFT buffer size, the system bandwidth is 80 MHz/512/8192=19.07 Hz.

The signal power from Ka and Q-band beacons are received and stored by a data collecting computer connected to the IDU’s serial port. The receiver software displays the actual receiving conditions and measurements; furthermore it handles the archive file system as well. The received power is collected and stored as raw data where daily measurement files are created. This data is post-processed to convert the received power to attenuation for later statistical analysis.

Initial stages of data processing (pre-processing) address the needs to validate the time series, discarding those with invalid data, and to eliminate as much as possible spurious measurements. These phases are of high relevance in order to guarantee the quality of the data. Data is considered invalid mostly due to loss of lock of the receiver, either because of rain attenuation exceeding the receiver margin, or because of some problem in the RF/IF stages.

Any received signal which shows fades or enhancements not related to propagation events are always eliminated from the measurements. Standard statistical analysis are then performed on the rain attenuations using post-processing programs and merge the monthly data to build long-term time series. The most important first order statistics are Cumulative Distribution Functions (CDFs), Complementary Cumulative Distributive Functions (CCDFs) that can be compared with the relevant ITU-R models.

Besides the beacon signal power measurement, we operate a meteorological station nearby the RF units to collect the rain rate, temperature, humidity and wind speed/direction data. In order to study the most important channel impairment, the rain attenuation the meteorological station is equipped with two different types of rain rate sensors: a tipping bucket one and a drop counter one. Nevertheless, the rain intensity sensors are located nearby of the receiver station. The reverse calculation using attenuation data to convert them to rain intensity is a different aspect to determine the rain intensity along the whole propagation path. In this way we get an averaged value of the rain intensity on the receiving path, therefore it provides an additional type of information about the characteristics of the meteorological circumstances. The reverse calculations are

Using Radio Wave Satellite Propagation Measurements for Rain Intensity Estimation

done by using the relating ITU-R P.618 methods as they are described in [1] and supported by further information like the recommendation ITU-R P.837 in [17].

III. ATTENUATION DATA VALIDATION WITH ITU-R

ITU-R P.618 [1] is basically used for comparing the statistics of measured rain attenuation with the ITU-R predictions. This model is a step by step procedure for the calculating rain attenuation cumulative function for satellite link. The recommendation provides the most accurate statistical estimate of attenuation on slant paths. This model is dividing the earth into five regions and assigning a rain rate to each region with the probability of the rain rate being exceeded. It can also be used for frequencies from 4 GHz-55 GHz and 0.01-5% percentage probability range. The model uses the rain rate at 0.001% probability level for the estimation of attenuation and then applies an adjustment factor to predict rain fade depth for other possibilities. Attenuation predictions requires first the estimation of a surface rain rate distribution and second the prediction of the radio wave attenuation value distribution, given by that the rain rate distribution. The model is derived based on log normal distribution, using similarity, principles. Inhomogeneities in rain, in both horizontal and vertical direction are accounted for in the prediction. The limit of the model is the data for years of measurements taken at the station and not all stations filled with the one-minute integration time requirement. In Figure 2 the diagram of the parameters for rain height calculation can be seen.

Recommendation ITU-R P.837 [17] contains maps of meteorological parameters that have been obtained using the European Centre for Medium-Range Weather Forecast (ECMWF) ERA-40 re-analysis database, which are recommended for the prediction of rainfall rate statistics with a 1-min integration time, when local measurements are missing.

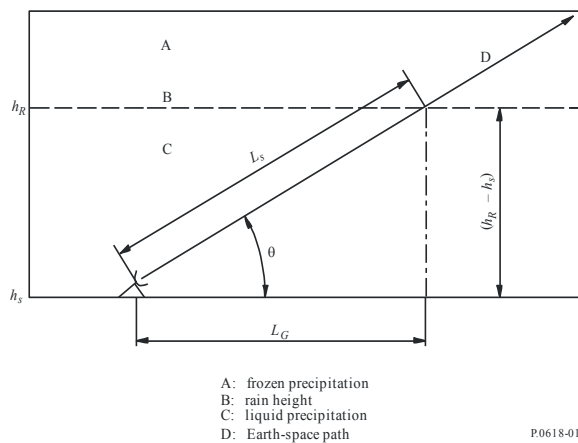


Figure 2. Rain height calculation based on ITU-R [2]

Rainfall rate statistics with a 1-min integration time are required for the prediction of rain attenuation in terrestrial and satellite links. Data of long-term measurements of rainfall rate may be available from local sources, but only with higher integration times. This recommendation provides a method for

the conversion of rainfall rate statistics with a higher integration time to rainfall rate statistics with a 1-min integration time.

Calculations can be made for link availability (%) for all frequency bands, to take into account link budgets, transmit power, receive sensitivity, antenna gain, target availability and other factors. Typical link availability Targets are 99.99%, 99.999% and higher.

Without detailing the above mentioned calculations in TABLE I. the most important values obtained from the calculations can be found:

TABLE I. INTERMEDIATE PARAMETERS FOR THE BUDAPEST STATION

R_{001} point rainfall rate	35.87 mm/h
Rain height h_R	2.95 km
Slant path length L_s	4.92 km
Satellite elevation (average)	35°
Effective path length L_E (Ka-band)	4.36 km
Effective path length L_E (Q-band)	4.72 km

Data processing is an essential phase of measurement data evaluation. The beacon receiver stations (at our station at BME as well) usually record the received signal's power. In order to get attenuation statistics, the received signal (power) should be converted to attenuation. This could be done by applying different methods, but they may influence the precision of the attenuation statistics estimation as well.

The first task is to overview the time series of the archived data to remove the invalid sections. As the measurement system is continuously operating, the unwanted power failures, external radiofrequency noise sources or due to maintenance works there could be invalid series of data in the recorded stream. Nevertheless, the goal of the operator is to keep the station working reliable in order to ensure the high availability.

The second data processing step is the conversion of the measured received power to attenuation. Therefore a key issue is the process of determining the clear sky level, as the reference level. Due to lack of a radiometer (as it is also at BME) the simplest method to apply is the long-term median or mean value of the received power time series as reference level. To take into account the long-term signal variations a more effective method is used to select manually the individual rain events [2].

As a first step in the data processing, invalid measurements are removed from the received signal of both attenuation and weather data using a combination of automatic and semi-automatic procedures, like visual inspection of the data. The data processing methodology is well described in [4] that have been partly applied for the actual measurement as well. A detailed process diagram can be found also in [4]. After this pre-processing the 0 dB reference level is identified by using a few minutes of data before and after each event and interpolating between them. This procedure, in combination with the lack of a radiometer, does not allow complete separation of cloud attenuation from rain so there will be some cloud attenuation included in the data. However, the highest cloud attenuation predicted by the ITU-R [2] (at the 1 % exceedance level) is 0.5 dB, thus the contribution should be

limited. Next, attenuation events are manually identified and selected for processing. The root mean square errors of the signal during clear sky conditions were calculated and the results verified with the models of ITU-R. The set of measurements to perform this evaluation in this paper covers the entire year of 2016.

IV. ANALYSIS OF CLEAR SKY ESTIMATION

One important parameter is the rain intensity for 0.01% of time, R_{001} , which is used for characterization of a given geographical location. According to the ITU regulations [17] its value is 35.87mm/h for Budapest location. However, this value may change during different time in years according to the local weather conditions. This could be one of the reasons why the measured and modelled curves are not exactly covering each other. To determine the clear sky level, the measured values are subtracted from the median (clear sky) received power and then calculated over an entire year. The attenuation events are mainly caused by rainy periods. The Complementary Cumulative Distribution Function (CCDF) of rain attenuation provides the probability of exceeding at different attenuation levels. The monthly distributions reveal how the rain events can significantly influence the actual weather conditions.

In Figure 3 the Complementary Cumulative Distribution Function (CCDF) of the measured attenuation for Ka and Q-band are depicted together with the distribution curves predicted by the ITU-R P.618 recommendation for an entire year of 2016. The clear sky level was estimated event-by-event bases using a visual inspection of the measured time series. This is a very time-consuming process, however this is a most reliable opportunity to estimate the clear sky level before and after the fade events. This method is applied almost by all of the members in the Alphasat propagation experimenters group [9]-[11].

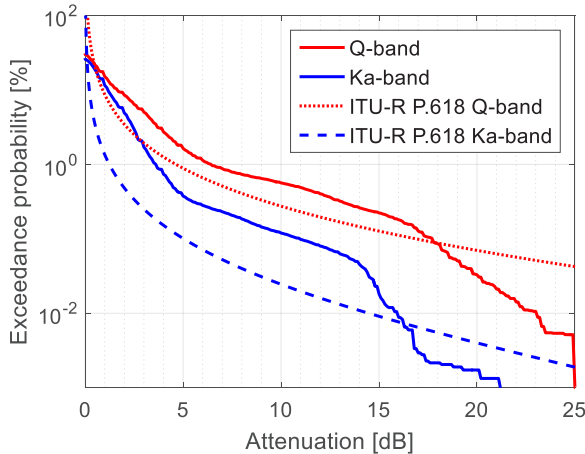


Figure 3. CCDF for Ka and Q band attenuation, manually selected events, compared with the ITU-R estimation

In order to estimate and enhance the clear sky level, of the error between measurements and the ITU-R model, the root mean square error (RMSE) has been applied as the square root of the expected value of the power of differences between the measured and ITU-R predicted values.

Figure 4 and Figure 5 are showing the RMSE for the Ka and Q bands.

We calculated the RMSE between the measured and the predicted attenuation values as the square root of the expected value of the power of differences between the measured and modelled values.

By applying the manually selected events and calculated the attenuation statistics (attenuation CCDF), we obtain the best approximation of the ITU-R curves.

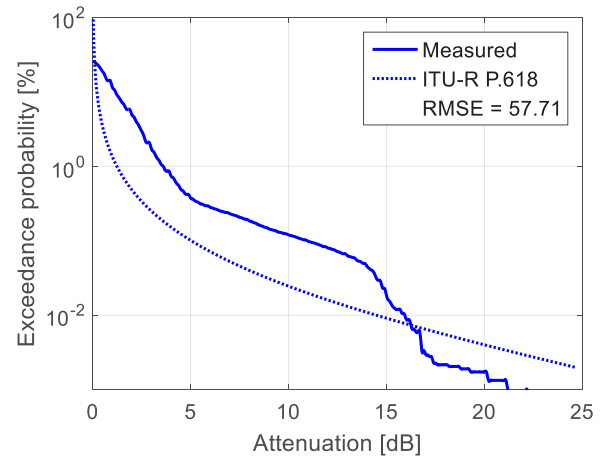


Figure 4. RMSE for Ka-band, clear sky level for manually selected events

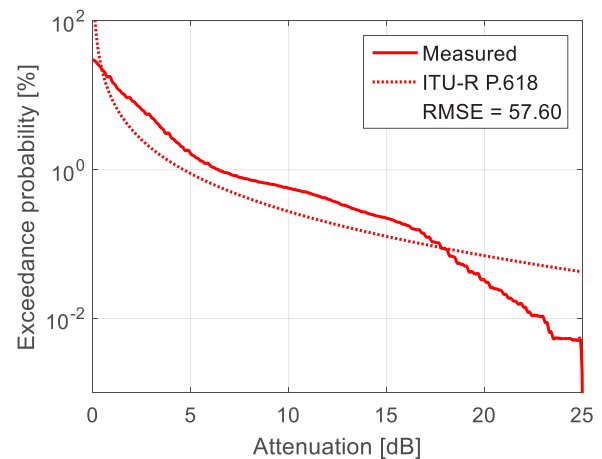


Figure 5. RMSE for Q-band, clear sky level for manually selected events

V. ESTIMATING THE RAIN INTENSITY USING ATTENUATION DATA

In the experimental propagation measurement station in Budapest rain rate is recorded by two different types of meteorological sensors. The data provided by these sensors are relating to the point rainfall rate at the receiver’s location. By applying the measured attenuation on the radio link to estimate the instantaneous rain intensity is a different approach to the problem. Similar work has been published in [14] using the

Using Radio Wave Satellite Propagation Measurements for Rain Intensity Estimation

ITU R P.838 recommendation, or with cellular mobile network data according to [15]. In the present work we apply the specific attenuation model for rain in the prediction of the rain rate, as a reverse calculation described in ITU R P.838.

The specific attenuation, using the frequency-dependent coefficients k and α given in Recommendation ITU R P.838 [16] can be expressed with the following power-law expression:

$$\gamma_R = kR^\alpha [dB/km] \tag{1}$$

For the Alphasat receiver station in Budapest these frequency-dependent parameters are the following:

	19.701 GHz	39.402 GHz
k	0.0924	0.4222
α	0.9987	0.8589

In the present case the inverse of Eq. (1) will be applied to calculate the rain intensity from the measured attenuation. The specific attenuation is the function of the measured attenuation A_m by dividing it with the effective path length as given in TABLE I. :

$$\gamma_R = A_m/L_E [dB] \tag{2}$$

By rearranging Eq. (2) the rain intensity in mm/h is as it follows:

$$R = 10^{\frac{\log(A_m/L_E) - \log(k)}{\alpha}} [mm/h] \tag{3}$$

Usually a beacon receiver is recording the beacon signal power level RP_m in dBm . The station in Budapest samples and stores the received signal power with $1/sec$ sampling rate. In order to express the momentary attenuation level from the received power the clear-sky level is required, that is the signal power when no rain attenuation arises. A simple approach to get the attenuation time series is applying the long term (monthly) median of received power as a clear-sky level. Unfortunately this method may not satisfactorily accurate as the median are influenced by the rainy and cloudy periods. The problem can be overcome if a radiometer is available at the receiver site that always provides the actual clear sky level, but at the Budapest receiver site no radiometer is installed. Therefore as it was shown in Section IV we used the best practice to select manually the attenuation events in order to determine the clear sky level for each of them. In this way the starting and ending of the event can be precisely determined and the temporal variation of the clear sky level can be eliminated. To overview the process Figure 6 depicts the measured attenuation time series and the rainfall rate calculated from the attenuation for both frequency bands. The rainfall rate measured with the tipping bucket sensor can be also seen in the figure. The figure is relating to July, 2017 that was a typical summer period with several rain events.

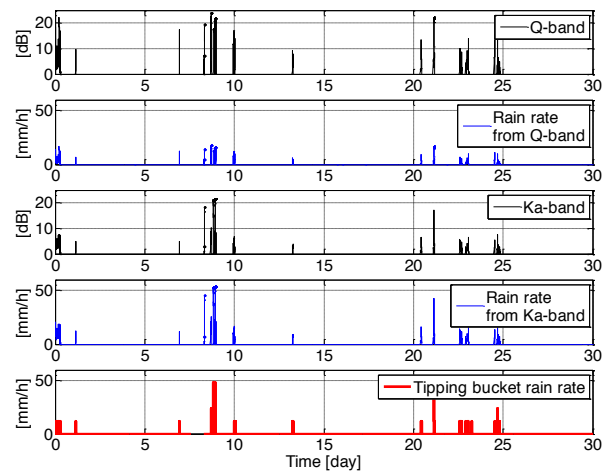


Figure 6. Rain rate calculated from the attenuation and the rain rate measured with tipping bucket sensor (07.2017)

For better observing the phenomenon an event with 50 minute duration has been selected and depicted in Figure 7.

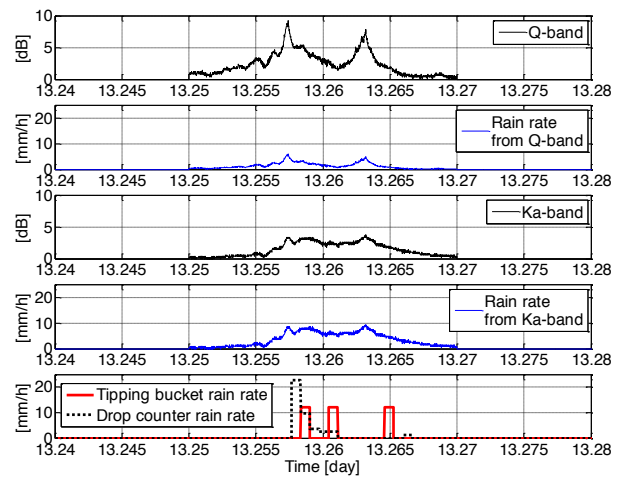


Figure 7. Selected rain event with calculated and measured rain rates (07.2017)

Although the tipping bucket sensor has been detected the event, due to its low resolution (0.2mm/tip) it cannot follow the shape of the rain attenuation event. The drop counter type sensor has better resolution (0.02mm) but it can be observed that it is still not capable to track the small signal variations.

Additionally, as the sensors are measuring only a point rainfall rate at the location of the receiver station, obviously we cannot expect a very good correlation with the rainfall rate that was determined from the path attenuation and that is relating to the full slant path between the ground station and the satellite. Another rain event with the relating measurements and calculations are depicted in Figure 8. The measured rain rate is graphed by using the drop-counter type sensor.

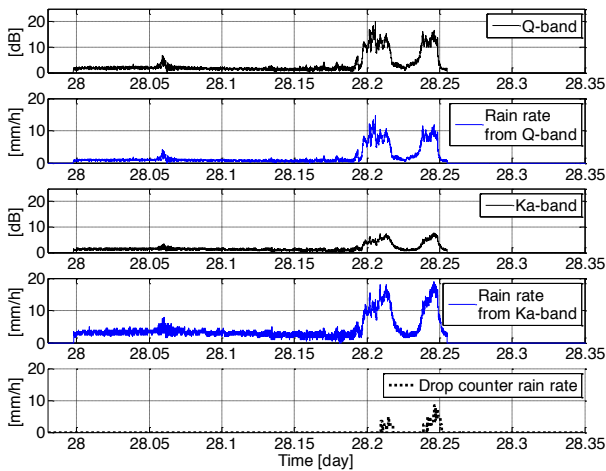


Figure 8. Rain event with calculated and measured rain rates (06.2017)

We may expect to get similar rain intensity values from both beacon signals as the measurement has been done at the same path and time. Nevertheless, by observing the figures one can see that the rain intensity calculated from the Ka-band signal attenuation is usually higher. As the effective path length calculation is including some long-term parameters originating from ITU-R databases frequency and polarization-dependent parameters are also applied. These circumstances may influence the calculations, and in order to clarify the exact reason of the deviation further investigations are planned.

Nevertheless, we have seen that the path attenuation may lead to a good estimation of the rainfall rate that is proportional to the precipitation along of the whole receiving path.

CONCLUSION

In this paper we have demonstrated how to convert the received power time series to attenuation time series, and it was further demonstrated that by selecting manually the rain events we achieve a good approximation of the statistics provided by ITU-R. We calculated RMSE errors for the comparison and to prove the results that were obtained.

The second part of this paper was dealing the conversion of the attenuation data to rain intensity. This method provides a different aspect to gain meteorological data by using radio wave signal attenuation measurements. Standard rain intensity sensors are always measuring point rainfall rates, while the proposed method is estimating the integral of the rain intensity along the propagation path that may lead to estimate the volume of the rain fields as well. This is a new approach to rain rate estimation that could be applicable not only for propagation engineers but also to specify meteorological measurements and it may help the better understanding of large-scale meteorological processes.

Future work is planned to cooperate with other European experimenters in order to compare co-existing data that may lead to a new rain field characterization method over a larger geographical area.

REFERENCES

- [1] ITU-R P.618-12, Propagation data and prediction methods required for the design of earth-space telecommunication systems, International Telecommunication Union, Geneva, Switzerland, 2015.
- [2] Bernard Adjei-Frimpong, László Csurgai-Horváth, "Estimation of Clear Sky Level for Satellite Propagation Measurements", H-SPACE 2018, 15-16 February, Budapest, Hungary, 2018.
- [3] Csurgai-Horváth L. et al., "The Aldo Paraboni Scientific Experiment: Ka/Q Band Receiver Station in Hungary", In Proc. 9th European Conference on Antennas and Propagation, Lisbon, Portugal, 12-17 April 2015J.
- [4] X. Boulanger, B. Gabard, L. Casadebaig and L. Castanet, "Four Years of Total Attenuation Statistics of Earth-Space Propagation Experiments at Ka-Band in Toulouse," in *IEEE Transactions on Antennas and Propagation*, vol. 63, no. 5, pp. 2203-2214, May 2015. doi: 10.1109/TAP.2015.2407376
- [5] János Solymosi, "SATCOM developments for ESA", H-SPACE 2017, 9-10 February, Budapest, Hungary, 2017.
- [6] T. Rossi, M. De Sanctis, M. Ruggieri, C. Riva, L. Luini, G. Codispoti, E. Russo, G. Parca, "Satellite Communication and Propagation Experiments Through the Alphasat Q/V Band Aldo Paraboni Technology Demonstration Payload," *IEEE Aerospace and Electronic Systems Magazine*, 31(3), 18-27, March 2016 doi: 10.1109/MAES.2016.150220.
- [7] Paraboni, A. Vernucci, L. Zuliani, E. Colzi, A. Martellucci: "A New Satellite Experiment in the Q/V Band for the Verification of Fade Countermeasures based on the Spatial Non-Uniformity of Attenuation", *Proceedings of EuCAP 2007*.
- [8] G. Codispoti et al., "Alphasat TDP5: AIT Activities on the Italian payload for communication and propagation experiments in Q/V band"; 17th Ka and Broadband Communication Conference 2011 Palermo, Italy.
- [9] A. Martellucci, J. R. Castro, G. Codispoti, P. Sivad and E. Benzi, "The ASI and ESA activities for the Alphasat Aldo Paraboni COMEX and SCIEX activities at Ka and Q/V bands," *2017 11th European Conference on Antennas and Propagation (EUCAP)*, Paris, 2017, pp. 1466-1470. doi: 10.23919/EuCAP.2017.7928789
- [10] V. Pek and O. Fiser, "Atmospheric attenuation analysis using aldo-Alphasat beacon signal in Prague," *2017 Conference on Microwave Techniques (COMITE)*, Brno, 2017, pp. 1-4. doi: 10.1109/COMITE.2017.7932356
- [11] J. Flávio, A. Rocha, S. Mota and F. Jorge, "Alphasat experiment at Aveiro: Data processing approach and experimental results," *2017 11th European Conference on Antennas and Propagation (EUCAP)*, Paris, 2017, pp. 2370-2374. doi: 10.23919/EuCAP.2017.7928330
- [12] J. M. Riera, D. Pimienta-del-Valle, P. Garcia-del-Pino, G. A. Siles and A. Benarroch, "Alphasat propagation experiment in Madrid: Results on excess and total attenuation," *2017 11th European Conference on Antennas and Propagation (EUCAP)*, Paris, 2017, pp. 1-4. doi: 10.23919/EuCAP.2017.7928777
- [13] S. Ventouras et al., "Large scale assessment of Ka/Q band atmospheric channel across Europe with ALPHASAT TDP5: The augmented network," *2017 11th European Conference on Antennas and Propagation (EUCAP)*, Paris, 2017, pp. 1471-1475. doi: 10.23919/EuCAP.2017.7928299
- [14] T. Hirano, J. Hirokawa and M. Ando, "Estimation of rain rate using measured rain attenuation in the Tokyo tech millimeter-wave model network," *2010 IEEE Antennas and Propagation Society International Symposium*, Toronto, ON, 2010, pp. 1-4. doi: 10.1109/APS.2010.5562253
- [15] A. Overeem, H. Leijnse, R. Uijlenhoet, 2011. Measuring urban rainfall using microwave links from commercial cellular communication networks, *Water Resources Research*, 47, W12505, doi: 10.1029/2010WR010350.
- [16] Recommendation ITU-R P.838-3, Specific attenuation model for rain for use in prediction methods, ITU, 2005

Using Radio Wave Satellite Propagation Measurements for Rain Intensity Estimation

- [17] ITU-R P.837-7, Characteristics of precipitation for propagation modeling, International Telecommunication Union, Geneva, Switzerland, 2017.



Bernard Adjei-Frimpong was born in Ghana. He received his MSc degree from (ESSIE) France and MTech from Cape Peninsular University of Technology in Electronics Systems and Electrical Engineering at Cape Town, South Africa in 2012. In 2016 he joined the Department of Broadband Infocommunications and Electromagnetic Theory at Budapest University of Technology as a PhD student in the area of millimeter-wave propagation through the atmosphere, with specific focus on rain attenuation measurements and modeling for satellite applications.



László Csurgai-Horváth is employed as an Associate Professor at Budapest University of Technology and Economics (BME), Department of Broadband Infocommunications and Electromagnetic Theory. His current research interests are focused on indoor and outdoor propagation, measurements and modelling of the rain attenuation on terrestrial and satellite radio links, time series synthesis and cognitive spectrum management. He has been involved in several international projects such as SatNEx, COST Action IC-0802 and QoS MOS. Recently, he has led some ESA-founded research projects relating to the Alphasat propagation and communications experiment and an ESA technology transfer demonstrator project for 5G indoor propagation measurements. Currently, he teaches space technology and channel modelling at BME in Budapest, Hungary.

Optical transfer in space communication

Andrea Farkasvölgyi and István Frigyes

Abstract— This paper presents the possibilities of Free-space optical connection (FSO) in space communication in case of satellite-to-spacecraft or satellite-to-satellite link. It summarizes the advantages and disadvantages of optical transmission in case of near-earth and deep space region. We present the most significant problems during FSO link application and introduce some techniques to eliminate the drawbacks. In this paper, we introduce the use of multi-channel FSO system, which is the most appropriate in order to maximize channel parameters with minimizing the transmission error. It compares available maximum channel parameters of near future space missions. Under special conditions in satellite-earth connection, the usage of the optical link may become very uncertain, because of the strong turbulent medium. We describe conditions under which the optical link can be applied in satellite communication and when it is necessary to effectively modify the optical connection. This article discusses the application of multichannel or more precise diversity systems, which we recommend for space communication.

Index Terms—FSO, satellite communication, atmosphere effect, space diversity, non-direct satellite links

I. INTRODUCTION

In space communications, the optical transmission has been applied since the mid-90s (SPOT-4 OPALE, OICET). This first inter-satellite optical communication link was a short distance, non-continuous operational transfer link between ARTEMIS GEO (Geostationary orbit) telecommunications satellite and SPOT-4 LEO (Low Earth orbit) Earth observation satellite. This inter satellite connection was a really high capacity data transfer link between two Earth's orbit (LEO-GEO 50Mbps, GEO-Ground 780Mbps). The structure of the system is shown in Fig.1.

The major challenge for an Earth observation satellite system is to transfer the collected data by observation equipment to a ground terminal. Due to the huge amount of data and since the satellite appears for about 10 minutes in each rotation period GEO repeater satellites are used [1] [2].

The FSO connections currently used in space communication are near-earth, near space, and deep space communication links. Near-earth communication links are ground-to-satellite or satellite-to-ground links, inter-satellite links, and interorbital links. So these connections are very short distance links (max ~80.000km) in contrast to the near space or deep space communication links.

The authors are with Department of Broadband Infocommunication and Electromagnetic Theory, Budapest University of Technology and Economics, Hungary; (e-mail: andrea.farkasvolgyi@hvt.bme.hu, frigyes@mht.bme.hu)

The International Telecommunication Union (ITU) defines deep space as a distance that is larger than 2 million km, so Moon-Earth distance and Lagrangian points L1 and L2 are still in near space. Comparing the near-earth and deep space communication, the extra path loss is minimum 60-80dB, this proportional to the square of the link distance [3].

In deep space communication, the goal is to maximize the transmission data rate, even if the frequency bandwidth is limited, because of the huge background noise. Due to the characteristics of long-distance or deep space communication channel, relative large transmission power, high receiver sensitivity, virtually error-free transmission and high-security channel are essentially required. In the case of near-earth and near space communication, the channel requirements are high data rate, consequently high bandwidth, and also high security [4] [5].

The article is structured as follows: We summarize in Chapter II the advantages and disadvantages of optical transmission. Chapter III includes the negative impacts to be addressed in inter-satellite and inter-spacecraft connections and the elimination and reduction techniques of these effects. In the second part of this chapter, we summarize the possible channel parameters for long-distance space optical links. Chapter IV is a brief analysis of mitigation techniques, possible coding, modulation and diversification options. The final chapter summarizes the possibility of minimizing the negative impact of the atmosphere.

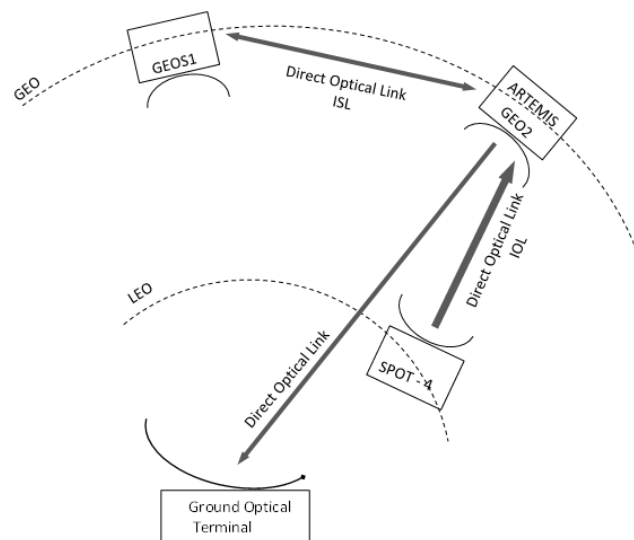


Fig.1 Inter Satellite Communication System; SPOT4 and ARTEMIS

II. ADVANTAGES AND DISADVANTAGES OF FREE SPACE OPTICAL COMMUNICATION

Compared the optical with the radio frequency (RF) communication, the differences come from dissimilar wavelengths. The regular wavelength for RF communication is between 30 mm to 3 m, compared to the optical 500nm - 1600nm. Therefore, RF wavelength is thousands of times larger than the optical wavelength. Differences due to diverse wavelengths are as follows.

A. Advantages of optical communication

Achievable high data rate: In RF and microwave communication systems, the allowable bandwidth is maximum 0.1%-5% of the carrier frequency, based on [27]. In optical communication, if the bandwidth is 1% of the carrier frequency, the allowable bandwidth will be 2THz. This makes the usable bandwidth at an optical frequency in the order of THz which is almost 50000 times that of a typical RF bandwidth. This results in high data rate due to high bandwidth and high effective isotropic radiated power (EIRP) because of the small divergence of the optical beam [3][4].

Lightweight and small size devices: In general, optical devices are much smaller and lighter than RF units. There is a big difference in the size of the radiation units (antennas and optical lens). The beam divergence is proportional to λ/D_R , where λ is the carrier wavelength and D_R the aperture diameter of the antenna or optical lens. The beam spread offered by the optical carrier is narrower than that of the RF carrier. This leads to an increase in the intensity of the signal at the receiver for a given transmitted power. Since the optical wavelength is very small, a very high directivity and large antenna gain can be achieved [6].

Free spectrum utilization: The optical system is free from spectrum licensing till now. This reduces set up and development cost [5][28].

High Security: In FSO communication no detection is possible without a professional instrument as result high directional laser beam with very narrow beam divergence [7]. In addition, the professional tool should be placed in the optical link to the illegal reception.

B. Disadvantages of optical communication

Required tight ATP system: The most fundamental disadvantage is the requirement of very tight acquisition, tracking and pointing (ATP) system due to the narrow beam divergence [5].

Effect of turbulence: FSO communication is dependent on varying atmospheric conditions that can degrade fatally the system performance. Therefore, the negative impact of turbulence must be considered near the ground, e.g. attenuation of fog, cloud, rain, dust etc [6].

Sun position: Another limiting factor is the position of the Sun relative to the laser transmitter and receiver. Solar background radiations can increase and that will lead to poor system efficiency [7].

Bandwidth limitation: In the case of long-distance communication it is necessary to apply bandwidth limited signal, it is about 0.1nm (1Å). Thus, the level of received noise can be reduced to a tolerable level [8].

III. CHANNEL CONDITION

The negative effects that influence the signal propagation are different in the turbulent atmosphere and in the free space environment. Thus, it is necessary to examine the two different environments: ground station-satellite and satellite-satellite connection.

A. Ground-to-space link

Various factors cause absorption and scattering in FSO system, but the major contribution for atmospheric attenuation is due to fog, clouds and water vapor. Eliminate the negative effect of different weather conditions that may perhaps cause huge losses is a fundamental objective. During dense fog conditions, when the visibility is even less than 50 m, attenuation can be more than 350 dB/km. Fog can extend vertically up to the height of 400 m above the Earth's surface, so the maximum attenuation due to fog is 140dB. Similar losses and other problems are caused by the cloud cover. Therefore the ground terminal is installed in a location where the probability of the problematic weather conditions (fog, cloud, water vapor) are small and its degree can be determined (based on reliable long-term measurement data) [6].

We should mention the powerful effects of the atmospheric turbulence. The channel parameters depend on the condition of the atmosphere. Basically, turbulence intensity can affect the probability of fade. If the receiving unit is provided with tight ATP system and the beam is collimated then the transmission channel parameter will be appropriate.

Beam wandering does not occur for downlink channels. However, for uplink at the satellite, it can be as large as several microradians. Beam wander can be mitigated by the use of multiple beams or a fast-tracking transmitter [5].

Pointing errors cause serious degradation in the communication channel reliability e.g. off-axis scintillation and deteriorate the outage probability. For downlink aperture averaging will occur for sufficiently large receiver apertures, but for uplink at the satellite, it does not occur this is why any receiver at the satellite always behaves like a point receiver.

Due to the presence of turbulence in the atmosphere, the laser beam wavefront arriving at the receiver will be distorted this effect is called angle-of-arrival fluctuation. This will lead to spot motion or image dancing at the focal plane of the receiver. For downlink, the rms (root mean square) angle-of-arrival fluctuations are several microradians, and for uplink at the satellite is generally less than 1 mrad [9].

Beam spreading causes a dilution of the available power for an uplink channel. Beam scintillation leads to redistribution of signal energy resulting in temporal and spatial irradiance fluctuations of the received signal. This intensity fluctuation of the received signal is known as scintillation and is the major cause of degradation in the performance of the FSO system.

The background noise has to be mentioned. The main sources of background noise are: diffused extended background noise from the atmosphere, background noise from the Sun and other stellar (point) objects and scattered light collected by the receiver. Typically in long-distance communication the background noise can be controlled by limiting the receiver optical bandwidth. Single optical filter with very narrow bandwidth in the order of approx. 0.01 nm

can be used to control the amount of background noise. Some of the design considerations while selecting narrowband optical filter are the angle of arrival of the signal, Doppler shifted line width of the laser and various temporal modes [10] [14].

B. Space-to-space link

Space FSO links are not subject to atmospheric and weather limitations, however, they are limited by other challenges like PAA (Point Ahead Angle), Doppler shift, acquisition and tracking, background radiations and satellite platform stability.

In that case when the transmitter and the receiver move relative to each other, the relative movement and the speed difference cause the Doppler shift. This problem must be compensated. Doppler shift is relevant in interorbital near-earth links and in deep space range also. For large distances, the Doppler shift rate is 70 to 100 times larger than in near-earth region. This means that in deep space communication the Doppler frequency shift rate is greater than the bandwidth.

PAA is one of the most critical parameters of the satellite-to-satellite or satellite-spacecraft laser communication that arises due to the relative angular speed of the two terminals. Due to the relative movement of the transceivers, the reflected signal is received with an offset relative to the beacon to hit the receiver in a suitable position. For the duration of the transmission (t_{n+1}) and the replies from the receiver (t_{n-1}), the angular movement of the receiving side: $PAA = \frac{2V}{c}$, where, V is relative speed of receiver to transmitter and c is light speed, see Fig.2. This is independent of the distance of communication, it only depends on the relative angular velocities (LEO track is 7km/s, compared with ~50km/s for Mars Earth). To do this, a scanning system is required to quickly scan the transmitter beam and receiver FOV (Field of View) [3][4].

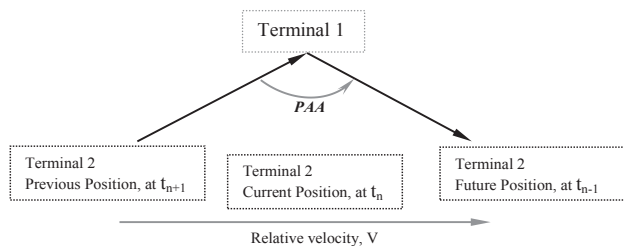


Fig.2 Most critical parameters in space communication, PAA

The Sun is the source of most background noise in the Solar System. It results in significant scattering if there is a strong background source close to the FOV (Field of View) of the receiver. Degradations caused by radiating celestial bodies other than the Sun are generally negligible except when receiving optics are directly pointing the Sun. The major source of background noise is due to scattering when an optical receiver design has its optics under direct exposure to sunlight [13] [14].

IV. CONNECTION CHARACTERIZATION

A. Near - earth link

The near-earth region is close to Earth. It means the Earth's orbits (LEO, MEO, GEO and HEO). These connections are characterized by achievable high data rate that is due to the high allocatable bandwidth. For such small distances, bandwidth limitation is not needed. For this region, the tight ATP system is required. The path loss can be compensated; the link delay is negligible compared to the deep space connections. Both direct and coherent detection links have been demonstrated in space-to-space links and space-to-ground links. Near-earth links have supported high data rates (> 1Gbps) from space-to-ground and 5.6 Gbps in space-to-space and ground-to-space links. Near-infrared wavelength lasers at discrete wavelengths around 800, 1064 and 1550 nm have been used.

In the case of space-to-space links, there is no negative effect of the atmosphere and weather conditions. Generally, phase coherent reception techniques are used that deliver high link capacity.

ESA (European Space Agency) has launched a complete and adapted program for support optical communication technologies, called Scylight (SeCure and Laser communication Technology) it is a project in the framework of ARTES, considering possible technologies, systems, and applications. Details about the program can be found on [29] and [30].

Based on recent research [31-33], the use of quantum technology provides tremendous opportunities for near-earth communication. Thus, the Scylight programme concentrates among others quantum cryptography technologies and initial services demonstration.

B. Deep space link

In space communication, the "long-distance" is usually used for distances of 0.1AU (Astronomical Unit) or more. Usually, the Moon as a celestial is the nearest target, which is already in that distance. In the near future, these links may be implemented in the form of fully optical systems.

In general, it is necessary to use the bandwidth limitation, it is about 1Å (0.1nm) [6], which reduces the background noise to an appropriate level. Tight ATP system is required similar to the shorter near-earth region. Exclusively IM/DD (Intensity Modulation / Direct Detection) is used, where modulations are OOK (On off Keying) for shorter links and PPM (Pulse Position Modulation) for deep space connections. The achievable data rate is strongly dependent on the link distance. For Mars communication, the maximum data rate may reach 0.5Gbps. The communication bands used are identical to the previous case [6] [10].

Let's summarize past and future missions using long-range optical connections. Well-known, full developed NASA mission was the Mars Laser Communications Demonstration (MLCD). It would have been a Mars-Earth high capacity system with RF and optical connections. But this project was suspended before the economic crisis.

NASA's new deep space project will launch in 2021. It is known as Psyche mission, Deep Space Optical

Optical transfer in space communication

Communications (DSOC). Psyche is the giant metal asteroid with near circular orbit between Mars and Jupiter.

The goal of this mission is to demonstrate at least a 10× enhanced data-return capacity relative to state of the art deep-space telecommunication systems with equivalent mass and

power; try to achieve 10 Mbps from Saturn and 250 kbps from Neptune by scaling flight transceiver to 0.4cm and 20W; a high-definition video stream transfer from deep-space and use of high data rate science devices [11] [12].

TABLE 1. Realized and future long-range optical space communication systems

Mission / instrument	Operation	Target	Link	Data rate (Mbps)	Distance (AU)	Q - Link difficulty dB 10log(Mbps·AU ²)
LLCD (Lunar Laser Com. Demonstration)	10. 2013 – 04. 2014	Moon –High band width, Lunar orbit to Earth optical link	Uplink	20	2.7E-3	-38.36
			Downlink	622		-23.43
OPALS (Optical PAYload for Lasercomm Science)	04. 2014 – 07.2014	LEO - From IIS to ground station	Up and Downlink	20-100	1.33E-5	-28.51 ÷ -77.52
LCRD (Laser Communications Relay Demonstration)	Flight in 2019	GEO/Near-earth and space High band width GEO to ground optical link	Up and Downlink	1200	2.68E-4	-40.64
DSOC (Deep Space Optical Communications)	Launch Summer of 2022; Arrival in 2026	Mars/Jupiter - Psyche mission, distance 0.1 to 2.5AU	Downlink	250	2E-1	10
			Downlink	250	5.5E-1	18.8
			Uplink	250	2E+0	30

Table 1. contains the maximum available channel characteristics at different systems and its range in astronomical units (1AU = 1.49 · 10¹¹m) [8] [15-20].

Table 1 introduces an added element of “difficulty” for optical links. Traditionally, the product of data rate and the square of link range (Mbps·AU²) is used as an index of link difficulty, however, for optical links the proximity to the Sun and the received background noise adds to the difficulty. Relative to near-earth, lasercom from deep space presents link difficulty that increases as the square of the link distance. For example, factors of 60–80dB additional gain will be required from Mars distances relative to GEO [8] [10].

V. REDUCTION OF NEGATIVE EFFECT OF ATMOSPHERE

As mentioned elsewhere, the basic requirements for space communication channel high data rate and also high security. Turbulence intensity can be reduced channel parameters; the characterization of turbulence is scintillation index. Strong turbulence results in large scintillation index; it is the effective variance of the incident signal [21-25].

Examine the use of multiple channels as a channel parameter correction technique. Using multiple channels system the scintillation can be drastically reduced with several multiple beams for uplink or downlink transmission. If the channels are presumably independent, the rate of decline is inversely proportional to the antenna numbers in the turbulent scenario.

In case of SIMO (single-input and multiple-outputs), these systems utilize the receiver diversity. Diversity gain is achieved by averaging over multiple signal paths. The signals can be combined at the receiver using selection combining (SC) or equal gain combining (EGC) or maximal ratio combining (MRC). Implementation of EGC is preferred over MRC due to its simplicity and suitable channel performance. In case of MISO (transmit diversity) a special space-time code such as optical Alamouti code is used.

As mentioned above, the result of using multiple channels at the ground terminal the scintillation can be reduced. The

degree of decline is 1/M or 1/N (M, N are the antenna number on transceiver of Earth's station). By the improving scintillation index, the channel parameter can also improve. For optical transmission from deep space, multiple receivers can be proposed for secure information transmission, since better channel parameters are available.

Usually, diversity techniques can improve the link performance. In case of the space-diversity the rate of increase in SNR can be determined as follows:

$$\langle \text{SNR}_M \rangle = \frac{M \langle I_{s,1} \rangle}{\sqrt{M(\sigma_{s,1}^2 + \sigma_{n,1}^2)}} = \sqrt{M} \langle \text{SNR}_1 \rangle \tag{1}$$

where the number of Earth's transceiver antennas are M and the degree of improvement is \sqrt{M} .

The negative effect of atmospheric turbulence can be reduced by installing receivers on high satellite orbit. Probably it would be a feasible signal reception from deep space by multiple simultaneous satellites receiver antennas. If onboard signal regeneration is available on satellites improved signal is radiated toward the ground terminal. Unfortunately, in the case of satellite-Earth connection, the use of optical links may become very vulnerable under special conditions. The effect of scintillation or attenuation, caused by the atmosphere degrades fatally the efficiency of the channel. That is why in certain cases an additional radio frequency link may be required by which negative effects of turbulence can be minimized. The biggest problem is that the maximum available bit rate of the RF or microwave link is much smaller than the original optical link. It would be a solution to transmit the optical signal by an inter-satellite-link to an orbital position where atmospheric conditions are appropriate for radiation of the optical signal toward the ground terminal. These systems would be a multi-hop communication channel that eliminates the negative effect of atmosphere and ensures the high data rate and high reliability, uninterrupted space link connection.

VI. CONCLUSION

This paper presented the properties of free space optical systems which used in space communication. We discussed the preferred properties and drawbacks of FSO in space communication. We presented the most significant problems in optical link application and introduced techniques for drawback eliminations. The paper detailed maximum available channel characteristics especially data rate and Q factor (link difficulty). In our article, the multi-channel application of optical systems was introduced by which maximize the channel parameters and minimize transmission error. Nevertheless, under special conditions, in the satellite to ground station relation, the usage of the optical link may become very uncertain. Usage of RF link reduces the negative impact of turbulence, but this would result in significant bandwidth reduction. An inter-satellite link would be the solution to this problem. Thus, the received signal can be radiated to an orbital position, from where atmospheric conditions are perfect toward a ground terminal. This is a multi-hop optical system that can decrease negative effects of atmosphere and weather conditions and ensures high reliability, uninterrupted space link.

ACKNOWLEDGMENT

The first author thanks Eva Godor for support and assistance.

REFERENCES

[1] T. T. Nielsen and G. Oppenhausser, "In-orbit test result of an operational optical intersatellite link between ARTEMIS and SPOT4, SILEX," Proc. SPIE, Free Space Laser Comm. Tech. XIV, vol. 4635, 2002.

[2] A. Katsuyoshi, "Overview of the optical inter-orbit communications engineering test satellite (OICETS) project," J. Nat. Inst. of Info. and Comm. Tech., vol. 59, pp. 5–12, 2012.

[3] H. Hemmati, A. Biswas, and I. B. Djordjevic, "Deep-space optical communications: Future perspectives and applications," Proc. IEEE, vol. 99, no. 11, pp. 2020–2039, 2011.

[4] H. Hemmati, Deep Space Optical Communication. John Wiley & Sons, New York, 2006.

[5] H. Kaushal, G. Kaddoum, "Optical communication in Space: Challenge and Mitigation Techniques". IEEE Communication Surveys and Tutorial, 2017

[6] B. Flecker, M. Gebhart, E. Leitgeb, S. S. Muhammad, and C. Chlestil, "Results of attenuation measurements for optical wireless channels under dense fog conditions regarding different wavelengths," Proc. SPIE, Atmospheric Opt. Model., Measure., and Simula. II, vol. 6303, 2006.

[7] A. Biswas, D.M. Boroson, "Near-Sun free-space optical communications from space," doi: 10.1109/AERO.2006.1655849 – Source: IEEE Xplore

[8] Yoza Shoji, et al., "A Pilot-Carrier Coherent LEO-to-Ground Downlink System Using an Optical Injection Phase Lock Loop (OIPLL) Technique," IEEE Journal of Lightwave Technology 2012.

[9] L. C. Andrews and R. L. Phillips, "Laser Beam Propagation through Random Media." SPIE Press, 2005.

[10] H. Kaushal, V. Kumar, A. Dutta, H. Aennam, H. Aennam, V. Jain, S. Kar, and J. Joseph, "Experimental study on beam wander under varying atmospheric turbulence conditions," IEEE Photon. Tech. Lett., vol. 23, no. 22, pp. 1691–1693, 2011.

[11] D.M. Boroson; Chien-Chung Chen; B. Edwards, "Overview of the Mars laser communications demonstration project" LEOS Summer Topical Meetings, 2005, INSPEC A. Num.: 8715041

[12] K. E. Wilson, "An overview of the GOLD experiment between the ETS-VI satellite and the table mountain facility," TDA Progress Report 42-124, Comm. Sys. and Research Sec., pp. 9-19, 1996.

[13] G. Baister, K. Kudielka, T. Dreischer, and M. Tüchler, "Results from the DOLCE (deep space optical link communications experiment) project," Proc. SPIE, Free Space Laser Comm. Tech. XXI, vol. 7199, 2009.

[14] Hemani, Kaushal, e.a "Ground-to-Satellite Optical Communication Link Performance with Spatial Diversity in Weak Atmospheric Turbulence." Fiber and Integrated Optics, ISSN: 0146-8030 print/1096-4681

[15] D. M. Boroson, A. Biswas, and B. L. Edward, "MLCD: Overview of NASA's Mars laser communications demonstration system," Proc. SPIE, Free Space Laser Comm. Tech. XVI, vol. 5338, 2004.

[16] A. Biswas, D. Boroson, and B. Edwards, "Mars laser communication demonstration: What it would have been," Proc. SPIE, Free Space Laser Comm. Tech. XVIII, vol. 6105, 2006.

[17] https://www.nasa.gov/sites/default/files/atoms/files/fs_dsoc_factsheet_150910.pdf, last visit Oct.8 2018.

[18] https://www.nasa.gov/sites/default/files/atoms/files/tglavich_dsoc.pdf, last visit Oct.8 2018

[19] Abhijit Biswas,* Hamid Hemmati, et al., "Deep-space Optical Terminals (DOT) Systems Engineering," IPN Progress Report 42-183, Nov 15, 2010 - https://ipnpr.jpl.nasa.gov/progress_report/42-183/183A.pdf

[20] Donald Cornwell, "Space-Based Laser Communications Break Threshold," Optics and Photonics News 27(5):24 doi: 10.1364/OPN.27.5.000024

[21] D. M. Boroson, A. Biswas, and B. L. Edward, "MLCD: Overview of NASA's Mars laser communications demonstration system," Proc. SPIE, Free Space Laser Comm. Tech. XVI, vol. 5338, 2004.

[22] A. Biswas, D. Boroson, and B. Edwards, "Mars laser communication demonstration: What it would have been," Proc. SPIE, Free Space Laser Comm. Tech. XVIII, vol. 6105, 2006.

[23] A. J. Hashmi, A. A. Eftekhar, A. Adibi, and F. Amoozegar, "Analysis of adaptive optics-based telescope arrays in a deep-space inter-planetary communications link between Earth and Mars," Optics Comm. (Elsevier), vol. 333, pp. 120–128, 2014.

[24] V. Weerackody ; A. R. Hammons ; D. J. Tebben, " Multi-Input Multi-Output Free Space Optical Satellite Communication Links," Information Sciences and Systems, 2007. CISS '07. 41st Annual Conference

[25] W. J. Hurd, B. E. MacNeal, G. G. Ortiz, and R. V. Moe et al., "Exo-atmospheric telescopes for deep space optical communications," in Proc. IEEE Aerosp. Conf., (Big Sky, MT), 2006.

[26] R. J. Cesarone, D. Abraham, S. Shambayati, and J. Rush, "Deep-space optical communications visions, trends, and prospects," in Proc IEEE Int. Conf. on Space Opt. Sys., (Santa Monica, CA, U.S.), 2011.

[27] Rec. S.1709-1 (01/07), in force

[28] ITU Radio Regulations, Geneva, 15 July 2016.

[29] <https://artes.esa.int/scylight/overview>, last visit Oct.8 2018

[30] <https://artes.esa.int>, last visit Oct.8 2018

[31] L. Bacsardi, On the Way to Quantum-Based Satellite Communication, IEEE Communications Magazine 51:(08) pp. 50-55., 2013

[32] Oi Daniel K L et al. CubeSat quantum communications mission, EPJ Quantum Technology, 4: Paper UNSP 6. 20 p. 2017

[33] Tamas Bisztray et al, "The Evolution of Free-Space Quantum Key Distribution" Infocommunications Journal X:(1) pp. 22-30. 2018



Andrea Farkasvölgyi received her M.Sc. electrical engineer from Budapest University of Technology and Economics. Currently, she is an assistant lecturer at Budapest University of Technology and Economics. Her research focuses on satellite communication, mutual channel techniques.



István Frigyes, D.Sc., he is Professor Emeritus at Budapest University of Technology and Economics. His research focuses on satellite communication, propagation effects and system aspects of microwave photonics. He led the Hungarian team of SATNEX and SATNEX-II. He was TPC member of ICCs, GLOBECOMs, he was the general chair of the 2007 IST Mobile Summit of the EU.

Comparing Calculated and Measured Losses in a Satellite-Earth Quantum Channel

Máté Galambos and László Bacsárdi

Abstract—Long distance distribution of quantum states is necessary for quantum communication and large scale quantum experiments. Currently this distance is limited by channel loss. Previous theoretical analysis [1] and proof of concept experiments [2] showed that satellite quantum communication may have lower losses than optical cable based counterparts. Recently the QuESS experiment [3] realized the first satellite-Earth quantum channel. In this paper we compare theoretical predictions of different mathematical models with experimental results regarding channel loss. We examine the HV-5/7 model, HV-Night model and Greenwood model of optical turbulences, the geometric [4] and diffraction [5][6] models of beam wander and beam widening. Furthermore we take into account the effect of atmospheric gases and aerosols as well as the effect of pointing error. We find that theoretical predictions are largely in the same order of magnitude as experimental results. The exception is the diffraction model of beam spreading where our calculations yielded only one tenth of the measured value. Given the ever changing nature of weather conditions and the changing composition of atmospheric aerosols we conclude that calculated and measured losses are in good agreement.

Keywords—satellite; quantum communication; channel loss; downlink;

I. INTRODUCTION

Quantum communication is the emerging field of sending and receiving messages using extremely weak signals. These signals could be single photons, coherent laser pulses or pairs of entangled photons. The signals are governed by quantum mechanics and thus behave fundamentally differently than classical counterparts.

One example of this unusual behavior is that unknown quantum bits cannot be observed or copied without running the risk of irreversibly changing them. These changes can later be detected revealing any eavesdropping attempt, which is extremely useful for cryptography. Another interesting property of quantum bits is that they can be entangled, meaning that their otherwise random behavior during measurement remains correlated even if they are separated by large distances.

These unusual behaviors allow for applications, which would not be possible otherwise. The most famous of these applications is quantum cryptography (cryptography with mathematically proven security [7][8][9][10][11]). Since quantum channels cannot be wiretapped without alerting the communicating parties, it is possible to distribute cryptographic keys on a quantum channel and check if there was an eavesdropping attempt. If the keys were compromised

The research is connected to COST Action CA15220 Quantum Technologies in Space. The research was supported by the National Research Development and Innovation Office of Hungary (Project No. 2017-1.2.1-NKP-2017-00001).

Máté Galambos is with Dennis Gabor College, Budapest, Hungary.

László Bacsárdi is with the Department of Networked Systems and Services, Budapest University of Technology and Economics, Budapest, Hungary

DOI: 10.36244/ICJ.2018.3.3

they are discarded. Otherwise they can be used to encrypt secret messages.

Other possible uses of quantum channels include sending two bits of data at the cost of sending a single quantum bit in a full duplex quantum channel (a method called superdense or quantum dense coding [14][15]). Other large scale experiments have also been proposed that require entangled photon pairs (such as experiments testing theories about quantum gravity [12][13]).

A good and detailed theoretical introduction to quantum information can be found in [14] while a more practical and communication centric introduction can be found in [15].

However, quantum communication requires long distance distribution of quantum bits. The distance at which quantum bits can be transmitted is currently limited by channel loss—either the loss of an optical cable or losses in free space. Experiments and theoretical works show that out of these two possibilities free space communication has lower losses. This motivated the race toward satellite-based quantum communication [16][17] which is currently unfolding even in the economic world of CubeSats [18][19].

The QuESS (Quantum Experiment at Space Scale) experiment realized the first satellite-Earth quantum channel. The satellite produced entangled photon pairs and transmitted them to two ground stations at Lijiang and Delingha China via two downlinks. The transmitters onboard the satellite produced photons in the near infrared range. This means that the equipment and communication resembles optical downlinks and not radio frequency transmissions.

In this paper, we compare theoretical predictions for channel loss with measured values. This is necessary because theoretical predictions of quantum communication are based on mathematical models describing classical light beams. This approach requires the assumption that properties of the atmosphere are either completely or at the very least largely independent of light intensity and that individual photons behave in a way that is consistent with an infinitesimal part of a classical light beam.

II. SOURCES OF LOSS IN SATELLITE-EARTH QUANTUM CHANNELS

Free space losses can be induced by multiple causes. In the following section we detail the sources of loss that we have taken into account in our calculations.

A. Pointing Error

Errors in targeting may result in the photon missing the detector and thus contribute to the free space channel loss. In our calculations we used the reported [3] value of the targeting error measured in the QuESS experiment and assumed that the targeting error had a Gaussian profile as reported [3].

In the QuESS experiment the detector mirror of the telescope was a Cassegrain reflector [3]. We approximated this in our calculation by assuming that the cross section of the

detector is a perfect circle with radius equal to the radius of the primary mirror and disregarded the blind spot created by the secondary mirror.

B. Beam Spreading and Beam Wander

Since the refraction of air is temperature dependent, fluctuations of air temperature can deflect and distort light signals. This effect depends on atmospheric conditions: the optical turbulence strength (denoted by C_n^2) is a parameter that describes the strength of these fluctuations. Higher C_n^2 values are associated with more beam widening and distortion. The magnitude of C_n^2 depends on wind speed, altitude and several other factors such as geographical features.

Atmospheric effects can also cause the center of a classical beam to wander. Higher C_n^2 values are also associated with more beam wander. It is worth noting that we do not distinguish between beam wander and beam spreading here, since in the long term time average the beam wander can be described as just another source of beam spreading. The beam widening is characterized by the radial beam divergence angle (or beam divergence for short) which is measured in micro-radians.

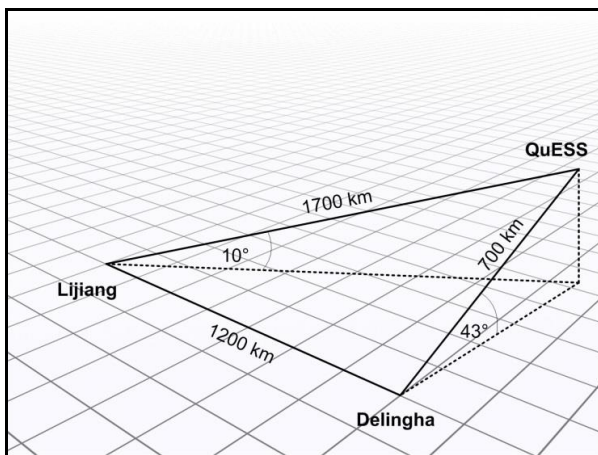


Fig. 1. Longest two-link distance between the satellite and the two ground stations.

C. Atmospheric Attenuation

Atmospheric gases and aerosols (solid particles of dust and liquid droplets) absorb and scatter light thus contributing to the channel loss. In our calculations, we took a semi-empirical approach. Instead of relying on purely theoretical calculations of molecular extinction we used experimentally measured values [20] of atmospheric transmittance.

This method is not only simple and easy to use, but it also gives us a more realistic picture of the aerosol profile as function of altitude than theoretical models. Since aerosol extinction is typically stronger than molecular extinction [20], we can expect a realistic result even with relatively inaccurate data about molecular extinction.

However, in these experiments [20] the wavelength was slightly different than in the QuESS experiment. Since aerosol extinction is mostly independent of wavelength (this statement is supported by both experimental data [20] and the theory of Mie-scattering [21]), we approximated aerosol extinctions by linear interpolation of measured values. In case of molecular extinction, we used the closest available analog which was a measurement performed using GaAs laser.

D. Efficiency of the Detector and the Optical Setup

Losses of the optical setup (due to imperfect detector efficiency, noise and inefficiencies in the photon generation process) are reported in the article [3] detailing the QuESS experiment. We have taken these efficiencies into account in our calculations.

III. CHANNEL LENGTHS AND ELEVATION ANGLES IN THE QUASS EXPERIMENT

An important factor in determining the channel loss is the relative position of the ground station and the satellite. The elevation angle as seen from the ground station determines the effective thickness of the atmosphere whereas the distance to the satellite determines the channel length. Therefore both of these parameters are required to estimate the channel loss.

The article describing the results of the QuESS experiment [3] focuses on two geometric arrangements. One is the moment when the communication is established and losses are the highest, and the other is when the overall two-channel length is the shortest and the channel loss is the lowest. In both cases the authors disclose either the channel length or the elevation angle but not both. However one can be calculated from the other.

We used the satellite - ground station - Earth center triangle to calculate the missing parameters. According to our calculations when communication was established (see Figure 1.) the satellite-Lijiang distance was 1700 km and the elevation angle at Lijiang station was 10°. At the same time the satellite-Delingha channel length was 700 km and the elevation angle at Delingha was 43°.

The combined two channel length was the shortest when the satellite was 800-800 km from both Lijiang and Delingha stations (see Figure 2.) and could be seen at 36° elevation angle from both ground stations.

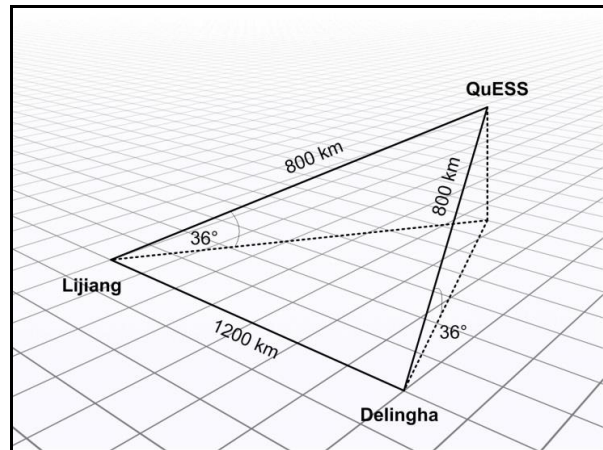


Fig. 2. Shortest two-link distance between the satellite and the ground stations.

It is worth mentioning that Figures 1. and 2. are merely illustrations and the triangles depicted on them are not proportional.

IV. OPTICAL TURBLUENCE

In order to model beam spreading and beam wander in the atmosphere we must know the atmospheric turbulence strength parameter (C_n^2). There are several different

Comparing Calculated and Measured Losses in a Satellite-Earth Quantum Channel

turbulence profile models to choose from – these are typically curves fitted onto measured data. Since free space quantum communication is carried out during the night (when the background noise is the lowest) we focused on models applicable to nighttime conditions. In our calculations we used three specific models. These are:

- Hufnagel-Valey 5/7 (or HV 5/7) model [22],
- HV-Night model [22],
- Greenwood model [22].

1) *HV 5/7 model*: The HV 5/7 is the most widely used model. It is a special case of the more general Hufnagel Valey model. According to the model the optical turbulence strength parameter C_n^2 is given by the following equation:

$$C_n^2 = 0.00594 \cdot \left(\frac{W}{27}\right)^2 (h \cdot 10^{-5})^{10} \exp\left(-\frac{h}{1000}\right) + 2.7 \cdot 10^{-16} \cdot \exp\left(-\frac{h}{1500}\right) + A \cdot \exp\left(-\frac{h}{100}\right), \quad (1)$$

where h is the altitude (measured in km), W is 21 [m/s] and A is $1.7 \cdot 10^{-14}$.

2) *HV-Night model*: The HV-Night model is another modification of the Hufnagel Valey model. In this model C_n^2 is given by the following equation:

$$C_n^2 = 8.16 \cdot 10^{-54} \cdot h^{10} \exp\left(-\frac{h}{1000}\right) + 3.02 \cdot 10^{-17} \cdot \exp\left(-\frac{h}{1500}\right) + 1.9 \cdot 10^{-15} \cdot \exp\left(-\frac{h}{100}\right) \quad (2)$$

3) *Greenwood model*: The Greenwood model was developed for astronomical imaging from mountaintops. It gives C_n^2 as

$$C_n^2 = [2.2 \cdot 10^{-13} (h+10)^{-1.3} + 4.3 \cdot 10^{-17}] \cdot \exp\left(-\frac{h}{4000}\right). \quad (3)$$

V. GEOMETRIC BEAM SPREADING MODEL

In this section we compare the calculated beam spreading with the measured values. The far field beam divergence has been reported to be 10 μ rad [3].

To calculate the beam wander we used the geometric approximation [4]. This treats optical turbulence as converging or diverging lenses. The radial beam divergence angle can be calculated as [4]:

$$\sigma_{\perp} = \left(2.92 \cdot D^{-1/3} \int_0^H C_n^2(h) \frac{\left(\frac{L_2(h)}{L}\right)^2}{\left|1 - \frac{L - L_2(h)}{F}\right|^{1/3}} dh \right)^{1/2} \quad (4)$$

where L is the total channel length, H is the altitude of the satellite, h is the altitude above ground level in the integration path and L_2 is the beam's slant path length corresponding to a given altitude. F is the focal range and D is the initial beam waist.

A. HV 5/7 Model

Calculating with the HV 5/7 model, the radial beam divergence comes out to be between 0.019 μ rad and 0.02 μ rad

depending on which transmitting telescope of the QuESS satellite was used.

The lower value of the calculated beam spreading corresponds to the larger telescope (0.3 m diameter) and the higher beam spreading angle corresponds to the smaller telescope (0.18 m diameter).

However, the dependence of beam spreading on channel length seems to be negligible (our calculations yielded approximately the same result for each downlink). The most likely explanation for this independence is that beam spreading is comparably small in vacuum. This means that the spot size at the detectors plane is mostly determined by the part of the optical path that is in the atmosphere.

This path length in the atmosphere is a function of the elevation angle. However a lower elevation angle corresponds to a longer link distance if the altitude of the satellite is fixed. The increase of the spot size seems to be almost perfectly cancelled out by the increase of the channel length and therefore the decrease of the angle corresponding to a given spot size.

Comparing the calculated and reported values we can conclude that these values are small—being several magnitudes smaller than the reported 10 μ rad [3] beam divergence.

B. HV Night Model

Using the HV Night model we obtain radial beam divergence angles between 0.009 μ rad and 0.01 μ rad.

The outcome of the calculation is similar to the previous model: the result is largely unaffected by channel length but depends on transmitter telescope diameter (the smaller beam spreading corresponding to the larger telescope).

Comparing measured and calculated values we conclude that the HV night model gives us results that are also several magnitudes smaller than the 10 μ rad radial beam divergence reported in [3].

C. Greenwood Model

Using the Greenwood model we get radial beam divergence angles between 0.16 μ rad and 0.17 μ rad.

The characteristic is similar to the previous models: the result is largely independent from channel length but depends on transmitter telescope diameter (the smaller beam spreading corresponding to the larger telescope).

Comparing the calculated and measured [3] values we conclude that the Greenwood model yields values roughly one tenth of the reported 10 μ rad beam divergence.

D. Comparing the Different Models

Comparing the measured beam spreading with the calculated values we can conclude that none of the optical turbulence models yield the measured result (see Figure 3.). Even the largest result is several magnitudes smaller than the reported value.

Figure 3. shows the calculated values of beam spreading and beam wander, measured in μ radians.

As we mentioned before, the QuESS satellite was equipped with two different transmitting telescopes. Black bars in Figure 3 indicate the beam wander/spreading in case of the smaller telescope (corresponding to more beam wander) and white bars indicate the beam wander/spreading in case of the larger transmitting telescope (corresponding to less beam wander). The bars are grouped by model.

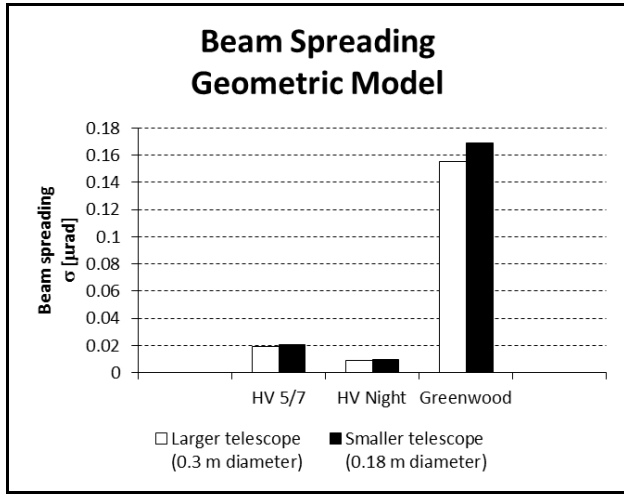


Fig. 3. Calculated values of beam spreading using the geometric model. The measured value was $10 \mu\text{rad}$ [3], which is significantly higher than the calculated values shown here.

VI. DIFFRACTION BEAM SPREADING MODEL

Another alternative to using the geometric beam wander model is a diffraction based model [5][6]. In this section, we present the results of our calculations using this approximation.

The radial beam divergence angle in the diffraction based model can be calculated as [5][6]:

$$\sigma_{\perp} = \arctg \left(\frac{1}{L} \cdot \left[\frac{4L^2}{k^2 D^2} + \frac{D^2}{4} \left(1 - \frac{L}{F} \right)^2 + \frac{4L^2}{k^2 \rho_0^2} \right]^{\frac{1}{2}} \right), \quad (5)$$

where L is the total channel length, F is the focal range, k is the wavenumber and D is the initial beam waist. ρ_0 is the phase coherence, which can be calculated as [5][6]

$$\rho_0 = \left[1,46k^2 \int_0^H C_n^2(h) \left(\frac{L_2(h)}{L} \right)^{5/3} dh \right]^{-3/5}, \quad (6)$$

where H is the altitude of the satellite, L_2 is the beam's slant path length that corresponds to a given h altitude (assuming a fixed elevation angle).

Since the elevation angle in the QuESS experiment was fairly low, we used Fante's approach to calculate the coherence length [6].

According to our calculations, the beam spreading should be between 0.86 - $0.87 \mu\text{rad}$. This is less than one tenth of the reported $10 \mu\text{rad}$ [3].

This result holds regardless of the model used for calculating the optical turbulence strength (see Figure 4.). The reason for the discrepancy between the measured and calculated value is currently unknown and warrants further investigation. Possible explanations include higher than expected turbulence or other factors not currently accounted for in our model.

VII. CHANNEL LOSS

Using the value of beam spreading measured in the QuESS experiment we can validate our method of calculating the channel loss. In this section we examine the channel loss when

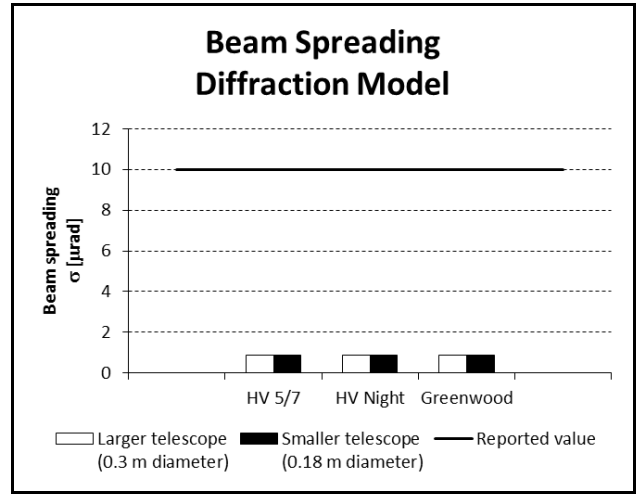


Fig. 4. Comparing measured [3] and calculated beam spreading using the diffraction model. Calculated values are a magnitude smaller than measured ones.

the combined two channel length is the longest (maximal loss) and shortest (minimal loss).

The results presented in this section are calculated assuming 50% overall optical efficiencies for the telescopes (while the actual value was reported to be somewhere between 45-55% [3]).

We calculated the channel loss as:

$$QTL = -10 \cdot \log_{10}(\tau_1 \cdot \tau_2) \quad (7)$$

where τ_1 and τ_2 are the effective transmittances of the two downlink channels (one to Lijiang and the other to Delingha). Each of these effective transmittances can be calculated as:

$$\tau_{1,2} = \tau_{P/S} \cdot \tau_{AE} \cdot \tau_O \quad (8)$$

where $\tau_{P/S}$ is the effective transmittance due to pointing and beam spreading, τ_{AE} is the transmittance due to atmospheric extinction, and τ_O is the effective transmittance due to other effects.

The value of τ_O comes from the reported [3] efficiency of the optical setup, detector efficiency and losses caused by background noise. The other two terms can be calculated using the following equations:

$$\tau_{P/S} = 1 - \exp \left(- \frac{R^2}{2 \cdot ((L \cdot \tan \sigma_{\perp})^2 + (L \cdot \tan \sigma_{\tau})^2)} \right), \quad (9)$$

where R is the detector radius at the ground station, L is the total link distance, σ_{\perp} is the radial beam divergence angle, and σ_{τ} is the targeting error (as reported in the QuESS experiment [3]).

Finally the atmospheric extinction can be characterized by:

$$\tau_{AE} = \sum_i \exp(- (s_i + k_i) L_i) \quad (10)$$

where L_i is the slant path length in the i^{th} layer of the atmosphere, whose aerosol and molecular extinction is given by s_i and k_i . (These values come from measurements [20]. We used data gathered during the summer, in the middle latitudes, under various weather conditions.)

Comparing Calculated and Measured Losses in a Satellite-Earth Quantum Channel

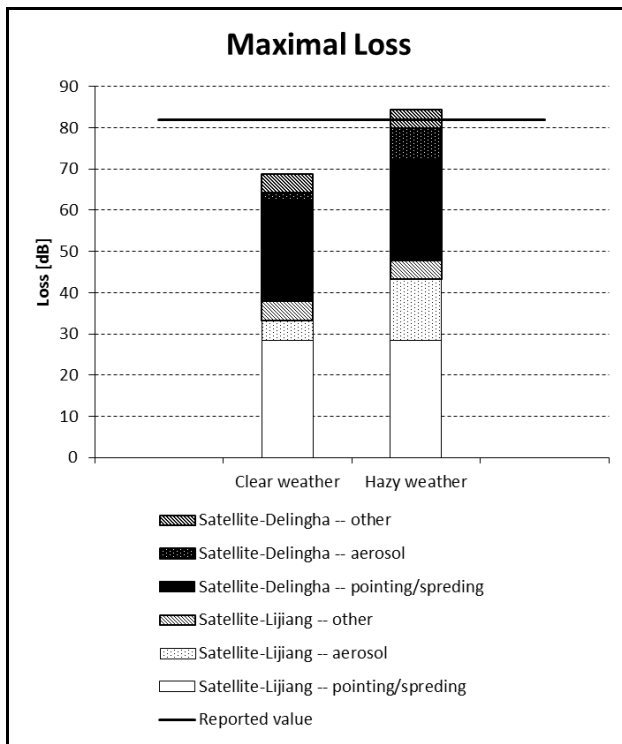


Fig. 5. Calculated and reported losses in case of the longest two-link distance in clear and hazy weather [3].

A. Maximal Loss

When the communication was established with the satellite (this situation is shown in Figure 1.), the measured two channel loss in the QuESS experiment was reported to be 82 dB [3].

According to our calculations, the loss due to pointing error, beam wander and beam spreading in the satellite-Lijiang channel was 28.54 dB while in the satellite-Delingha channel it was 24.36 dB. The combined two channel loss due to beam spreading and pointing error was 52.9 dB. These values are denoted by white and black bars in Figure 5.

(Note that the values of beam spreading are unaffected by weather conditions; these bars are equally high regardless of whether the weather is clear or hazy.)

According to our calculations, the channel loss due to molecular and aerosol extinction had to be between 4.85 dB and 14.72 dB in the satellite-Lijiang channel (depending on weather conditions). In the satellite-Delingha channel, the loss had to be between 2.05 dB and 7.68 dB. (See the dotted bars in Figure 5. Note that these losses can significantly differ based on weather conditions.)

Taking into account all factors (including optical and detector inefficiencies) the total combined two channel loss had to be between 68.92 dB (assuming clear weather) and 84.43 dB (assuming hazy weather). These calculated values are in good agreement with the reported 82 dB loss [3] (which is shown as a horizontal line in Figure 5.).

B. Minimal Loss

Losses were the lowest when the satellite was closest to the two ground stations (see Figure 2.). The measured two channel loss in this position is reported to be between 64 dB and 68.5 dB [3].

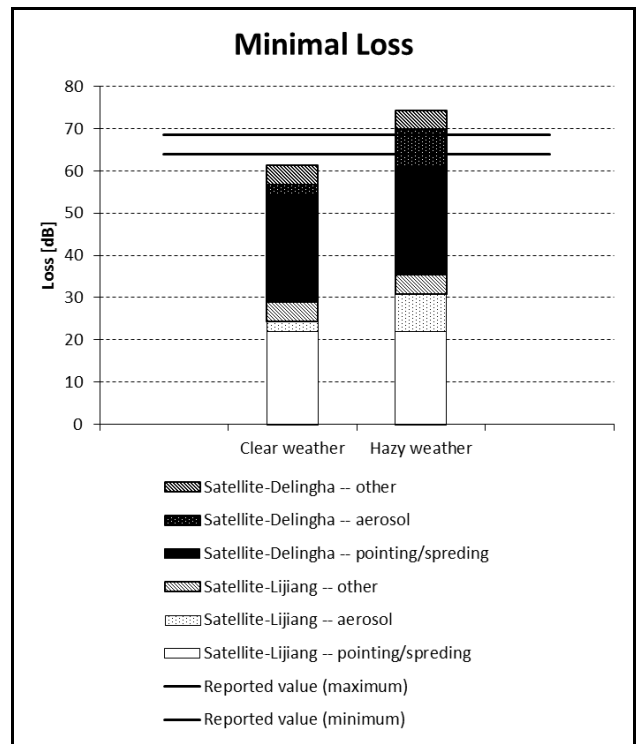


Fig. 6. Calculated and reported losses in case of the shortest two-link distance [3].

According to our calculations the loss due to pointing error, beam spreading and beam wander had to be 22 dB in the satellite-Lijiang channel and 25.52 dB in the satellite-Delingha channel. These losses are shown as black and white bars in Figure 6.

(Note that these losses do not depend on weather conditions. However they do depend on the ground station, or to be more precise the detector mirror size at the ground station which differed in this case.)

The combined two channel loss caused by beam spreading comes out to be 47.53 dB.

According to our calculations, the channel loss due to molecular and aerosol extinction had to be between 2.38 dB (assuming clear weather) and 8.91 dB (assuming hazy weather) in both channels.

(Note that aerosol extinction is not affected by the detector. This type of loss depends only on the elevation angles—which happened to be equal in this case—and the weather conditions.)

Taking into account all errors, losses and inefficiencies the combined total two channel loss had to be between 61.41 dB and 74.47 dB. These calculated values are in the same order of magnitude as the measured 64 to 68.5 dB reported in the literature [3]. (These values are represented as solid horizontal lines in Figure 6.)

VIII. CONCLUSIONS

In this article, we compared the measured beam spreading and channel loss of the QuESS satellite experiment [3] with calculated values.

We found that our calculations yield significantly lower beam spreading than the reported value [3]. However calculating with the reported value of beam spreading, we

obtained losses that agreed with measured losses.

The exact result of beam spreading in our calculations depends on the model of optical turbulence strength being used. We examined the HV 5/7 [22], HV Night [22] and Greenwood [22] models of optical turbulence.

We also examined the geometric optics model [4] and diffraction model [5][6] of beam spreading. Our calculations yielded results that are several magnitudes smaller than that of the reported values [3]. This relationship holds true for all models of optical turbulence strength and all models of beam spreading.

The reason for this discrepancy is currently unknown and warrants further investigation. Possible explanations include stronger than expected turbulence or other unexpected factors not currently present in our model.

Furthermore, we compared reported and calculated losses. The reported losses of a quantum channel in the QuESS experiment were roughly between 60 dB and 85 dB [3]. According to the literature [22], these losses are in the same order of magnitude as the total link loss of a classical satellite-to-ground laser communication channel.

However for quantum channels, other authors [23] estimated the channel loss to be significantly lower than the value reported in the QuESS experiment [3].

To perform our calculations, we used the measured value of beam spreading as reported in [3] instead of our calculated beam spreading. The results we obtained this way were in good agreement with the reported data.

We performed these calculations in two particular cases: the first was when communication was established with the satellite, and the combined two-channel length was the longest (see Figure 1.), and the second was when the satellite was closest to the two ground stations and the two-link distance was the longest (see Figure 2.). In both of these cases we examined clear and hazy weather. Our results show that the reported loss was between the calculated values obtained simulating clear and hazy weather (these correspond to lowest and highest loss respectively). This means that given the correct beam spreading the rest of the model is likely accurate. This accuracy can be further tested by comparing more calculations with more experimental data.

REFERENCES

[1] J.P. Bourgoin, et al., "A comprehensive design and performance analysis of low Earth orbit satellite quantum communication," *New Journal of Physics*, vol. 15, iss. 2, p.023006, 2013.

[2] A. Zeilinger, "Long-distance quantum cryptography with entangled photons," *Quantum Communications Realized*, vol. 6780, p. 67800B. International Society for Optics and Photonics, 2007.

[3] J. Yin, et al., "Satellite-based entanglement distribution over 1200 kilometers," *Science*, vol. 356, iss. 6343, pp.1140-1144, 2017.

[4] J.H. Churnside, and R. J. Latatits, "Wander of an optical beam in the turbulent atmosphere," *Applied Optics*, vol. 29, iss. 7, pp. 926-930, 1990.

[5] H.T. Yura, "Atmospheric turbulence induced laser beam spread," *Applied optics*, vol. 10, iss. 12, pp.2771-2773, 1971.

[6] R.L. Fante, "Electromagnetic beam propagation in turbulent media: an update," *Proceedings of the IEEE*, vol. 68, iss. 11, pp.1424-1443, 1980.

[7] C. H. Bennett, G. Brassard, "Quantum cryptography: Public key distribution and coin tossing," in *Proc. IEEE Int. Conf. Comput., Syst. Signal Process.* New York, NY, USA, pp. 175-179, 1984.

[8] D. Gottesman et al., "Security of quantum key distribution with imperfect devices," *Quantum Inform. Comput.*, vol. 4, iss. 5, pp. 325-360, 2004.

[9] V. Scarani et al., "The security of practical quantum key distribution," *Rev. Modern Phys.*, vol. 81, iss. 3, pp. 1301-1350, 2009.

[10] V. Scarani, R. Renner, "Quantum Cryptography with Finite Resources: Unconditional Security Bound for Discrete-Variable Protocols with One-Way Postprocessing," *Phys. Rev. Lett.*, vol. 100, iss. 20, pp. 200501

[11] L. Gyongyosi, S. Imre, "Information Geometric Security Analysis of Differential Phase Shift Quantum Key Distribution Protocol," *Security and Communication Networks*, vol. 6, iss. 2, pp. 129-150. (2013)

[12] S.K. Joshi, et al., "Space QUEST mission proposal: experimentally testing decoherence due to gravity.," arXiv preprint arXiv:1703.08036. 2017.

[13] D. Rideout, et al., Fundamental quantum optics experiments conceivable with satellites—reaching relativistic distances and velocities. *Classical and Quantum Gravity*, 29(22), p.224011, 2012.

[14] M. A. Nielsen, I. L. Chuang, "Quantum Computation and Quantum Information: 10th Anniversary Edition," New York, Cambridge University Press, 2010.

[15] S. Imre, L. Gyongyosi, "Advanced Quantum Communications: An Engineering Approach," Hoboken, New Jersey, Wiley-IEEE Press, 2012.

[16] L. Bacsardi, "On the Way to Quantum-Based Satellite Communication," *IEEE Communications Magazine*, vol. 51, iss. 8, pp. 50-55, 2013.

[17] T. Bisztray, L. Bacsardi, "The Evolution of Free-Space Quantum Key Distribution," *Infocommunications Journal*, vol. X, iss. 1, pp. 22-30. 2018.

[18] D. Koi et al, "Cubesat Quantum Communications Mission", *EPJ Quantum Technology*, vol. 6, iss. 4, 2017.

[19] R. Grieve et al, "SpooQySats: CubeSats to demonstrate quantum key distribution technologies", *International Astronautical Congress 2017*, Adelaide, Australia, IAC-17,D5,4,4,x38936

[20] R.A. McClatchey, R.W. Fenn, J.A. Selby, F.E. Volz, and J.S. Garing, "Optical properties of the atmosphere," (No. AFCRL-72-0497), Air Force Cambridge Research Labs, Hanscom Afb Ma. 1972.

[21] M. Bass, "Handbook of Optics. 2.," New York : McGraw Hill Professional, ISBN: 978-0-07-163314-7. 2010.

[22] A.K. Majumdar, J.C. Ricklin, "Free-Space Laser Communications Principles and Advances," New York : Springer, ISBN 978-0-387-28652-5. 2008.

[23] M. Aspelmeyer et al., "Long-distance quantum communication with entangled photons using satellites", *{IEEE} J. Sel. Topics Quantum Electron.*, vol. 9, iss. 6, pp.: 1541-1551, 2003.



Máté Galambos studied at the Budapest University of Technology and Economics (BME) as an Engineering Physicist. He completed 264 out of 300 credits until 2014, when he left without a diploma. Currently, he is studying as a Computer Engineer at Dennis Gabor College. Previously he worked as a Guest Research Assistant at École Polytechnique Fédérale de Lausanne, Switzerland, where he studied the electron structure of doped single wall carbon nanotubes using EPR methods. Currently he works as a Junior

Research Assistant at BME, Budapest, Hungary. His present research focuses on quantum informatics and quantum communications. In 2011 he received Best Paper Award at the ICQNM 2011 conference, France, for his paper "New Method for Representation of Multi-qubit Systems Using Fractals". In 2013 he won first prize at the OTDK student conference, and the same year he won the Society of Pro Scientia Medalists' Special Prize for Outstanding Scientific Contribution.



László Bacsárdi received his M.Sc. degree in 2006 in Computer Engineering from the Budapest University of Technology and Economics (BME). He wrote his PhD thesis on the possible connection between space communications and quantum communications at the BME Department of Telecommunications in 2012.

From 2009, he works at the University of Sopron, Hungary (formerly known as University of West Hungary). He holds an associate professor position at the Institute of Informatics and Economics, University of Sopron. He is Research Fellow at the Department of Networked Systems and Services, BME. His current research interests are quantum computing, quantum communications and ICT solutions developed for Industry 4.0. He is the Vice President of the Hungarian Astronautical Society (MANT), which is the oldest Hungarian non-profit space association founded in 1956. Furthermore, he is member of IEEE, AIAA and the HTE as well as alumni member of the UN established Space Generation Advisory Council (SGAC). In 2017, he won the IAF Young Space Leadership Award.

Ontology based Indoor Navigation Service for the ILONA System

Dániel Péter Kun, Erika Baksáné Varga and Zsolt Tóth

Abstract—An ontology based way finding algorithm is presented in this paper that allows route generation between two separate parts of an indoor environment. The presented ontology provides a flexible way to describe and model the indoor environment, in addition it fits and extends the existing model of the ILONA System. Ontology reasoners provide an efficient way to perform complex queries over the knowledge base. The instances, that are queried by the reasoner, are used to initialize the graph which represents an indoor environment. Due to parameterization of the reasoner, different graphs can be generated from the ontology which makes the way finding algorithm flexible. Thus, the task of indoor way finding was converted into a well-known graph search problem. Dijkstra’s shortest path algorithm is used for route generation in the graph yielded. The algorithm was implemented and tested in the ILONA System and its functioning is demonstrated by real-life scenarios.

I. INTRODUCTION

Indoor positioning systems aim to find people or objects inside a building. The interest in this topic grows with the widespread use of smartphones in modern society. Multiple solutions use the sensors commonly found in an average smartphone. The existing solutions differ in the technology and heuristics used and in the costs. Although the first indoor localization system was developed in the early 1990’s, there is no common solution for indoor positioning unlike the Global Navigation Satellite Systems for outdoor environment.

Availability, cost and accuracy are the key criteria during the development of an indoor positioning system. The most recent solutions consider smart phones as client device due to their low cost and wide range of sensors. Thus, Bluetooth, ultrasound and WiFi RSSI are all popular technologies for indoor positioning. Every technology differs in cost and precision. WiFi RSSI based solutions have very low installation cost because they use the communication network that is already established, but these systems usually achieve only about 3 meter accuracy. Apple’s iBeacon and Estimote beacons are based on Bluetooth technology and an accuracy of 1-4 meters could be achieved with this technology depending on the location’s size. Finding a precise and cost-efficient, while widespread technology is a challenge for the developers even nowadays.

Indoor navigation systems are built upon indoor positioning systems and extend their functionality in the same way as outdoor navigation systems make use of the service provided by global positioning systems. For example, Global Navigation Satellite Systems use the Global Positioning System to determine and track the users’ location and a navigation software such as iGo or Waze for way finding and navigation. Malls, airports, hospitals often place floor plans to facilitate the indoor way finding for their visitors. Despite the popularity of this technique, it has numerous drawbacks. Firstly, it is an offline solution and it has to be replaced when the environment changes. Secondly, the poster size grows with the size of the building so its applicability is limited. Thirdly, finding of a specific location in a huge floor plan could be difficult and may take a long time. On the other hand, online indoor navigation systems can deal with the above challenges. Although updating of the map would require

Daniel Péter Kun, Erika Baksáné Varga and Zsolt Tóth are with the Institute of Information Science, University of Miskolc, Hungary
 {kun3.vargae,tothzs}@iit.uni-miskolc.hu

DOI: 10.36244/ICJ.2018.3.4

TABLE I: Comparison of ontology-based semantic location models

Name	Usage of Ontology	Application Rules
LOC8	space model ontology, context model ontology, sensing model ontology	spatial relationship rules
OntoNav	user navigation ontology, indoor navigation ontology	path selection rules
Onalin	user navigation ontology, indoor navigation ontology	path selection rules, user preferences
Smart Hospital Project	entities ontology, semantic locations ontology, physical locations ontology	sensing areas rules
ILONA	indoor navigation ontology	path selection rules, restrictions

some modifications on the server, the zooming in the floor plan is a simple task because there are software libraries to solve this problem. Finally, searching with an online application is quite simple and it would increase the availability of the indoor navigation system.

The ILONA (Indoor Localization and Navigation) System [16] is a web-based indoor navigation system developed at the Institute of Information Science, University of Miskolc, Hungary. The aim of the system is to provide a common research environment for evaluation and testing of positioning and way-finding methods. ILONA System can be used to provide way-finding services for students, employees and visitors between and inside the buildings located in the university campus which occupies a continuous territory of approximately 350.000m² (85 acres) including 25 buildings.

The paper presents a case study that demonstrates the applicability of the ontology created for storing semantic information for indoor navigation.

A. Related Works

Indoor navigation has shown numerous applications. One of the best examples is robotics, where the system relies on the sensors found in the machine. Other well-known applications are smart hospitals, exhibitions and e-commerce. All of these systems perform functions specific to their own field. Since navigation information in indoor environments is more than geo-information, researchers have been proposing the addition of semantic models to offer suitable representations and applications. Map-based indoor navigation systems are straightforward implementations of global navigation applications in indoor environment. Map-based systems can use their own indoor representation of the building [13] or standard modeling tools. IndoorGML provides a standard format for modeling indoor environments, for example it was used to model educational buildings in [7]. One group of semantic models is based on ontology. This section introduces the existing systems [1], [2], [14], [18] using ontologies. Table I summarizes the ontology-based semantic location models based on [17] extended with the ILONA ontology.

1) *LOC8*: LOC8 [14] is a location model and extensible framework for programming with location. The whole framework contains three models that are called context model, sensing model and space model. These models are expressed by ontologies, which provide API to describe and apply context information into the location-based services. The space model represents the locations with a relative location, a symbolic representation and a geometric region. The context model represents the additional layers of information that belong to the locations that can be used for further reasoning. The sensing model maps information about the traversing entities of the model (e.g. people). LOC8 is based on the OWL API and the Protege ontology editor.

2) *OntoNav and ONALIN*: OntoNav [1] is a semantic indoor navigation system and an ontology framework for handling routing requests. User Navigation Ontology (UNO) and Indoor Navigation Ontology (INO) are Knowledge Models in the OntoNav System. UNO reuses and extends some concepts of existing ontologies, like GUMO [5]. INO serves as the model for both the path searching and the presentation tasks of the system. Based on UNO and INO, path selection rules described by SWRL (Semantic Web Rule Language) could discard some paths which are physically not accessible for users, and identify paths which match users' preferences.

The system consists of a navigation service, a geometric path computation service and a semantic path selection service. The navigation service serves as the main connection between the user and the system, receiving the requests of the user and returning the optimal path for him. The geometric path computation service is responsible for the calculation of the physical paths for the user. This is handled with classic graph theory. The semantic path selection service handles the decision about the best available path. This module compares the available path with the profile and the requests of the user then the module returns the optimal solution.

ONALIN [2] is the extension of the OntoNav system with the American Disability Act. Good examples for this extension includes height of stair and handrail availability.

3) *Smart Hospital Project*: The smart hospital project [18] was created to represent mobile entities in a navigational model within medical facilities. Its model consists of atomic location, semantic location and physical location. Physical locations detail the current whereabouts of the mobile entity, while semantic locations describe the environment through identifiers like door, room, floor, building, etc. The atomic location connects the two previous models through detailed information gathered by positioning techniques.

B. ILONA System

Our global motivation is to launch a Smart University Project (similar to the Smart Hospital Project) that takes into consideration the preferences of university employees, students and visitors. The test site of the initial project is the University of Miskolc (Hungary) with 1000 employees, 15 thousand students (approximately 1% disabled, 1% foreign language speaker) and thousands of visitors.

This project needs a system that integrates location and navigation services. Map-based systems use only geo-information, while ontology-based systems can also make use of semantic information related to indoor spaces. The design and implementation of the ILONA System [16] was performed in view of these requirements. As a consequence, the navigation component can use an ontology-based model, similar to ONALIN.

The main difference between this model and the one that we propose in the present paper is the approach to user preferences in path selection. ONALIN lets users add their preferences concerning the route (e.g. I want to use the elevator). Our inverse approach does

not presume apriori knowledge about the indoor facilities. Users can declare their restrictions by specifying what they do not want to or cannot use (e.g. I cannot use the stairs) and the system provides all alternative ways to reach the destination. In this way, for example, the hanging wheelchair lift instead of the handrail stairs will not be disregarded. In other words, the semantic model of the ILONA system applies restrictions, rather than preferences, when making decisions. Consequently, we do not need to have any apriori knowledge about the building's facilities, therefore the ontology does not include special annotations. Users can give their "negative" preferences and the system will automatically exclude these gateways from the route. Any other alternatives will be displayed. If an invalid restriction is given, for example the user states that he does not want to use elevator and there is no elevator in the building, this request is ignored.

The ILONA System [16] was designed and developed to provide a flexible framework to test and compare various indoor positioning and navigation methods. The component based architecture and the loose coupling of services allows the extension of the system with various algorithms. The main subsystems are the measurement, positioning, navigation and tracking modules that are shown in Figure 1. These components are developed individually. The measurement subsystem defines the data model [15] of the fingerprinting database and provides web services for the managing of measurements. The positioning subsystem is a collection of various indoor positioning methods and it is continuously expanding with novel implementations. The tracking subsystem provides a service for observation of the users' movements. This paper focuses on the navigation subsystem of the ILONA System.

While the ILONA System defines the component structure and the web interfaces that invoke services whose expected behavior is also defined, the concrete implementation of these services is delegated. In this way the system can be extended with a novel way finding algorithm in three steps. Firstly, the novel algorithm has to be defined in a class that implements the corresponding interface. Secondly, the library that contains the novel method has to be added to the web component. Finally, the web component has to be configured to use the new method. Because of its flexibility and the services already provided, the ILONA System is chosen to implement and test the way finding method presented here.

The extension of the ILONA System with an ontology based navigation service allows the comparison and analysis of indoor navigation and way finding algorithms. Due to the component based architecture of the ILONA System, the navigation and positioning algorithms can be analyzed, tested and evaluated independently. In addition, the design of the ILONA System facilitates its extension and reconfiguration. Thus, ILONA System provides a common environment for the development and comparison of indoor positioning and navigation methods. Consequently, we can consider the way finding algorithm presented in this paper as a reference for other way finding methods.

C. Goals

The goal of the present research was the extension of the ILONA System with an ontology-based way finding method. Three major challenges occurred during the design of the module. Firstly, the ontology should fit to the existing data model of the ILONA System that is used and defined by its other components. Secondly, the way finding algorithm had to be designed. Finally, the implementation of the navigation module should not affect the other existing components. In addition, the suggested way finding algorithm and its implementation demonstrates the flexibility and extendability of the ILONA System.

The way finding algorithm is the major contribution of the paper. The applied ontology model allows the adaptation of the navigation

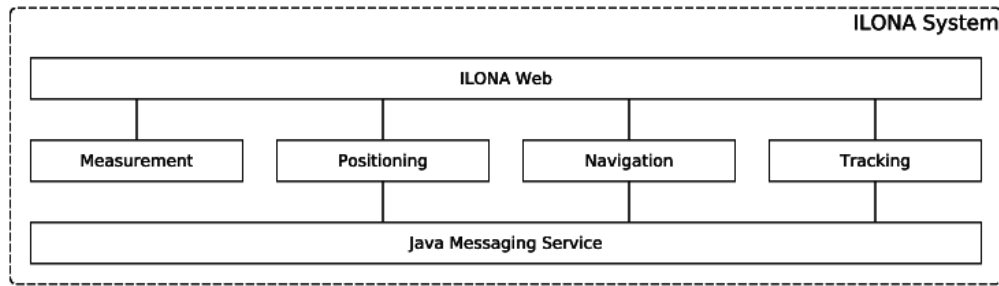


Fig. 1: Subsystems of the ILONA System [16]

system to arbitrary indoor spaces such as transport stations, shopping malls, educational buildings and offices. In addition, this algorithm can be used as a reference during the development of other indoor navigation algorithms. Because simplicity was kept in mind during the design, the way finding method can be improved with the application of different graph search algorithms.

II. METHODS

The hiding of technical details, the extension of the existing model, parameterizability and support of the administrator were set as the main criteria about the ontology-based navigation service. The ILONA System was designed to be as general as possible so it provides only an abstract navigation service to the end users. Hence the system can work with both ontology- and map-based way finding algorithms. Due to this abstraction, hiding the ontology and other technical details is necessary. The ILONA System provides data types for modeling measurements and position information. The data model of the navigation module and its ontology [8] should fit to the existing model [15]. In addition, the navigation module requires additional information to model the indoor environment properly. As a consequence, the data model of the navigation subsystem should be extended. The presented ontology introduces the concept of gateways that represent the connection between two zones. The ontology-based way finding algorithm should be configurable and able to generate different routes based on various restrictions. The navigation module defines a general set of restrictions that can be chosen by the users in order to omit certain types of gateways. For example, a disabled person could generate a route that avoids stairs. Although the ontology-based navigation service should be transparent for end users, administrators should be able to manage the ontology and other parameters of the way finding algorithm. In order to facilitate the administrator's work the ontology-based navigation component should provide some services intended to be used by administrators only.

Design and development of the navigation module of the ILONA System has three major challenges. Firstly, the navigation module has to extend the existing data model of the ILONA System without its modification. Since a well-defined function set is assigned to each module, this can only be modified via extension based on the Open-Closed Principle. This requirement makes the design of the navigation component challenging. Secondly, the navigation subsystem should use the positioning service of the ILONA System which is assumed to be provided. Although the behavior of the positioning service is defined by its interface, neither the performance nor the accuracy of the positioning service is given. Because the navigation service relies on the positioning service, its performance and accuracy may depend on the actual positioning algorithm. This dependency could make the testing and evaluation of the navigation service difficult. Finally, the

design of the navigation module has to fit well to the existing modules. The designed ontology-based way finding method deals with the above challenges and can be integrated to the ILONA System. In addition, the ILONA System can provide services for route generation in arbitrary indoor areas such as shopping centers, transport stations or office buildings. The next sections provide detailed information about the design and development of the navigation service in the course of which all three challenges were taken into consideration.

A. Ontology Model

Navigation models in ubiquitous computing should involve context information reflecting the semantics of the actual application. Navigation context expresses the state transitions of entities in the navigation route. The ontology-based modeling approach is a semantic way of organizing and sharing context knowledge augmented with advanced reasoning capabilities for processing context information [17].

The ontology model of the Navigation component of the ILONA System is based on the concept of Zone which is a closed, disjunct section of the indoor space. Each zone is named and uniquely identified, and denotes an arbitrary area with no specific dimensional restrictions. The exact spatial and dimensional definition of each zone comes from the measurement component of the ILONA System. Zone entities are connected by Gateways – like elevators or stairs – which are also modeled as entities. By definition, gateways are named and uniquely identified, closed and disjunct indoor areas having the role of connecting zones. In this way the graph representing a navigation route consists of nodes denoting Zones and Gateways. This simple representation allows for flexible modeling of indoor environments. The routing algorithm should find a way between two Zones by determining the sequence of Zone and Gateway nodes to go through.

Gateways are modeled as entities because in this way attributes can be assigned to them (e.g. permission of use). Consequently, they are represented as nodes in the navigation graph where residence can be registered (e.g. getting stuck in an elevator). A gateway may connect more than two zones. This many-to-many relationship between the zones through the gateways is modeled by two has_a relations: a zone may have multiple exit gateways (from) and it may also have multiple entrance gateways (to). Either of these relationships can be omitted to represent a one-way gateway (e.g. cashier's desk as exit from supermarket). Following the VOWL notation [9], Figure 2 illustrates the possible navigation routes between two zones (Ground floor lobby and Room 109) in the building of the Information Technology Institute at the University of Miskolc, Hungary. The figure shows gateways as hatched nodes and extends the navigation path with the one-way emergency exit.

There are five gateway types defined in our model at present: doors, elevators, escalators, stairs and virtual gateways. This list can be extended with other facilities on demand. Doors are separators between

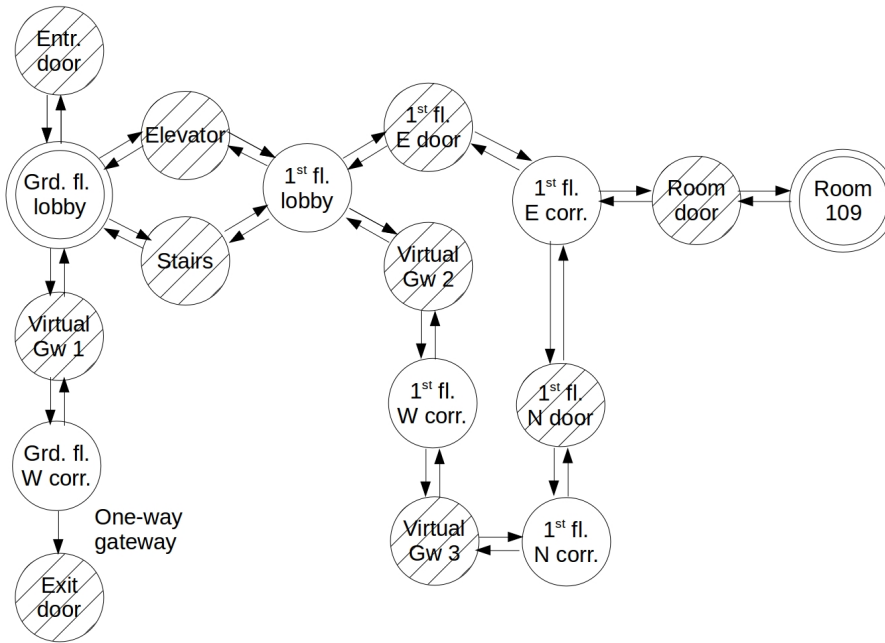


Fig. 2: Navigation route model between zones

zones with small physical extension, i.e. their dimensions are not considered in the computations. Elevators, escalators and stairs have considerable dimensions and they are differentiated according to their attributes (e.g. accessibility). In the case of virtual gateways, the connection between the zones is established through non-physical objects (e.g. joint corridors not separated by doors).

For modeling complex indoor spaces the possibility of grouping zones is necessary. The greatest zone group defined in our model is "building". This is comprised of several other zone groups which can be established on the basis of various criteria, e.g. location, functionality or ownership. For example, the floors of the building are zone groups according to location containing neighboring zones. The laboratories of the Automation Department reside in the western corridors of the ground and 2nd floors. Although these are not neighboring zones, they belong to the same zone group when dividing the zones according to ownership. Generally speaking, the grouping of zones must comply with the following rules:

- 1) Each zone is a member of one or more zone groups.
- 2) A zone group may have any number of other zone group members.

This model was inspired by the Composite design pattern [3], where zone groups are composites of zones representing recursive part-whole hierarchies (see Figure 3).

B. Ontology Definition

In computer science, the term "ontology" was introduced by Gruber [4] to mean "the specification of a conceptualization". This is a formal description of the concepts (entities with their attributes) and the relationships that exist in a given domain. The ILONA navigation domain ontology can be accessed via Protege [12], the web-based ontology editor that assists the creation and manipulation of ontologies. The knowledge representation language used for ontology

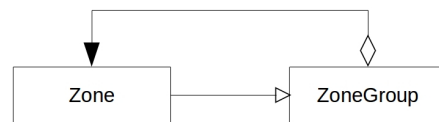


Fig. 3: The modeling of zone groups

construction is the Web Ontology Language (OWL 2) [10]. It provides classes, properties, individuals, and data values on the syntax level. OWL ontologies are mapped to RDF graphs and stored as RDF documents.

The first task in ontology creation is to define the taxonomy of classes described by various attributes. In the ILONA ontology the top-most classes are Gateway and Zone with two attributes: name and id, where id refers to a value coming from the measurement component of the ILONA system. The five gateway types are implemented as subclasses of the Gateway class. The ZoneGroup class is derived from the Zone class and in order to represent zone groups as composites of zones an auxiliary class should be introduced to denote their relationship. This ZoneGroupMembership class connects each zone to a zone group. Since ZoneGroup is the derived class of the Zone class, this implies that zone groups can be members of other zone groups. Our model specifically defines two subclasses of the ZoneGroup class: Building and Floor to demonstrate the recursive part-whole hierarchy of floors in buildings. The proposed ontology model has not been fully implemented yet. As mentioned above, the grouping of Zones is possible according to several criteria apart from location (e.g. functionality: offices, laboratories, corridors, etc.; ownership: departments, faculties).

Ontology based Indoor Navigation Service for the ILONA System

The second task is to define the relationships between the classes other than specialization. In the ILONA ontology the most important object properties are those that define the entrances and exits of zones via gateways. By default, each zone may have zero or more entry and exit gateways, so the `from_zone` and `to_zone` object properties are not restricted. For modeling zone groups as composites of zones through the `ZoneGroupMembership` class, two additional membership relations are defined: `has_zone` and `has_zonegroup`. Technically, these object properties implement the many-to-many relationship between zones and zone groups.

Figure 4 shows the ILONA ontology drawn by OntoGraf which is a visualization tool embedded in Protege-5.0.0 desktop edition [12]. The presented ontology contains only physical zones, zone groups and gateways, and the figure shows only the taxonomy of classes without attributes in order to emphasize only the major concepts. Continuous line blue arrows represent has subclass relations in the taxonomy. Dashed arrows are for those object properties that are explicitly defined. Between the `Zone` and `Gateway` objects the yellow arrow denotes the `to_zone`, while the red arrow denotes the `from_zone` property. The `to_zone` property is used to express that 'a specific gateway leads to a given zone'. On the other hand, the `from_zone` property states that 'an actual gateway is an exit from a given zone'. Since OWL ontologies allow only one-to-many (parent-child) relations, the many-to-many relationship between the `Zone` and `ZoneGroup` objects should be converted to two has type object properties (denoted by dashed arrows) the domain of which is the `ZoneGroupMembership` technical entity.

C. Ontology Generation

The presented navigation module provides some functions for the administrators in order to facilitate the configuration of the ontology used. The structure of the indoor environment is stored in a knowledge base whose model is defined by the ontology [8]. Although the data model is given, the knowledge base has to be populated with instances that is time consuming. Moreover, the `Zone` object stored in the ILONA System should be mapped to a corresponding instance of the ontology. Manual insertion of these objects is not just time consuming, but may cause errors and mismatches. To reduce the probability of mismatches and to facilitate the population of the knowledge base, an ontology generation service is defined that initializes the structure of the knowledge base and inserts the records from the database of the ILONA System.

The ontology generation process is shown in Figure 5. The administrator sends an HTTP request to the server to ask for the initial knowledge base. The HTTP request is processed by the controller layer of the navigation module that parses and validates the request. Valid requests are forwarded to the `OntologyGenerationService` that implements the business logic. The initialization of the knowledge base consists of two major steps that are the querying of the `Zone` objects and the population of the knowledge base.

In the first step, the `Zone` objects are queried via HTTP from the controller of the measurement module of the ILONA System. During the query, the request is also parsed and validated then forwarded to the corresponding service that uses Data Access Objects to manipulate the database. Data Access Objects hide the technical details of the storage from the service. The current version of the ILONA System supports only MySQL database that is manipulated via JDBC. The objects queried from the database are converted by the Data Access Objects and forwarded to the service. The service returns with a collection of the objects that are marshalled to JSON format and sent back to the navigation module as a HTTP response.

In the second step, the queried `Zone` objects are used to populate the knowledge base. The `persist` component of the navigation module is used to initialize an empty knowledge base from the ontology template that is stored on the server. After that the `Zone` objects are inserted into the temporary knowledge base and then the temporary file is sent back to the administrator via HTTP by the controller. At the end of the process, the initialized knowledge base containing ontology instances is stored on the administrator's computer and it is ready for further modification.

D. Way Finding Algorithm

The navigation module of the ILONA System defines services for way finding but its implementation is delegated. Thus, the users and the developers have a different view of the system. From the user's point of view, the ILONA System always provides the desired service via the same path and its expected behavior is defined. From the developer's point of view, the ILONA System provides a bunch of functions and facilitates for the development, publishing and testing of different way finding algorithms. In other words the ILONA System can be extended with various way finding algorithms while its behavior remains the same.

The presented way finding algorithm traces the routing problem back to a well-known graph problem and uses the ontology to store graphs whose number grows combinatorially with the number of nodes. Figure 6 shows the sequence diagram of the route generation process. From the user's point of view, the way finding service is a black box whose input are the source, the destination and the restrictions. The way finding service returns with a sequence of zones that defines the path between source and destination. Way finding is a complex process that consists of three major steps: querying from the ontology, route finding in the graph and conversion of the path to zones.

In the first step, the ontology is used to query the navigation graph. The user sends the source and destination along with a list of restrictions to the server. The corresponding web controller processes and validates the request, then calls the way finding service. The way finding service uses the `OntologyDAO` to filter the gateways based on the restrictions. Filtering is performed by an ontology reasoner and its results are used to populate a `ZoneMap` object that encapsulates a graph. Nodes of the graph store only the zone identifier.

The second step is responsible for way finding. Because `ZoneMap` is a graph whose nodes are the zones, and the edges represent the gateway connections between the zones, the way finding problem can be solved with graph algorithms. The edges are unweighted in the graph because the navigation service does not calculate time or distance estimation for taking the route between the source and destination zones in the present stage of the research. On the other hand, finding the right gateway could be challenging. Dijkstra's Shortest Path algorithm is commonly used to find a path between two nodes in a graph whose cost is minimal. Since the weights of the edges are equal, the shortest path will be the one that has the minimum number of edges. In other words, the way finding algorithm will return with a path that contains as few gateways as possible.

In the final step, the path found is converted to a list of `Zones` and presented to the user. The way finding algorithm returns a sequence of `Zone` identifiers. The way finding service has to query the `Zone` objects by their identifier. To query `Zone` objects, the service performs HTTP requests to the corresponding web controller of the measurement subsystem. The way finding service returns with a list of `Zone` objects queried. The way finding controller marshalls these objects into JSON format and send them to the user in a HTTP response. The further processing and visualization of the generated route is not part of the current research.

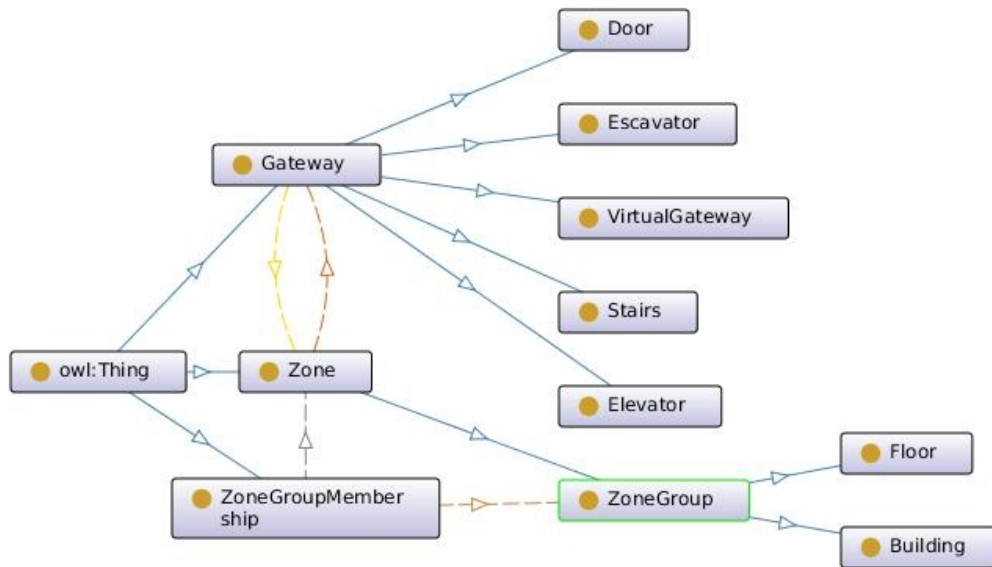


Fig. 4: Ontology structure

III. RESULTS

The ontology-based indoor way finding method was implemented as a part of the ILONA System. The implementation was tested on unit, component and integration levels. In addition, real-life case studies were used to demonstrate the applicability of the proposed way finding method.

A. Implementation of the navigation subsystem

The navigation subsystem is one of the major elements of the ILONA System. The implementation of the way finding algorithm required the modification and extension of some modules in the navigation subsystem, but these modifications were limited to the current subsystem. Furthermore, modifications had to fit the module structure of the ILONA System.

Figure 7 shows the module structure of the navigation subsystem and the modifications. The model module has been extended with classes for modeling the indoor environment. Modification of the service module was not required during the implementation. The service-impl module has been added and it defines the way finding algorithm. The algorithm is enclosed into a class that implements the WayFindingService interface so it can be easily integrated to the ILONA System. The way finding algorithm extracts data from the ontology that is stored in the file system. The storage and query functions related to the ontology are defined in the persist, and implemented in the persist-ontology module. Although the controller module has been extended with the ontology generation controller, the way finding service controller was not modified.

The model module defines the domain objects and implements a low level business logic such as value validation. The ZoneMap class represents a graph that is used for way finding. The graph data structure is provided by the JGraphT Java library that allows the modeling of any kind of graphs. The general graph representation of JGraphT was adapted to the ILONA System by the ZoneMap class. Hence the nodes of the graph adapted by ZoneMap store Zone

objects. The instantiation of ZoneMap is performed by classes of the persist-ontology module.

Persistent storage of the domain object is defined in the persist and implemented by the persist-ontology module. Due to the separation of definition and implementation, the modules became loosely coupled and they could be developed independently. In addition, all ontology related program code was limited to the persist-ontology module. The OWL API [6] was used to represent and manage ontology entities. Querying and data extraction were performed with the HermiT Reasoner [11] that facilitates the execution of complex queries. These queries are composed on the basis of the restriction set given by the user. Based on the restrictions, the reasoner returns with the edges that are allowed.

The way finding algorithm was implemented in the service-impl module. The algorithm is enclosed into a class that implements the WayFindingService interface of the service module. Thus, the algorithm can be used via the interface in other modules that facilitate the configuration of the ILONA System. The algorithm queries the graph nodes and edges that fulfill the restrictions from the ontology via the OntologyDAO interface that is defined in the persist module. Query results are used to initialize a ZoneMap object that is used to find the shortest path between the source and destination zones. When the ZoneMap returns with a list of zone identifiers, the algorithm queries the corresponding Zone objects. So the way finding algorithm returns with a list of zones that describe the route generated.

The web services are stored in the controller module that is responsible for the processing and validation of HTTP requests and invocation of the service methods. The web controllers are mapped to certain URL path and wait for requests. Request parameters and the yielded response data are represented in JSON format. Consequently, the navigation component can be integrated with any kind of client devices.

Figure 8 details these components and their connections according to the N-Tier Architecture. The Presentation Tier is called Web Tier,

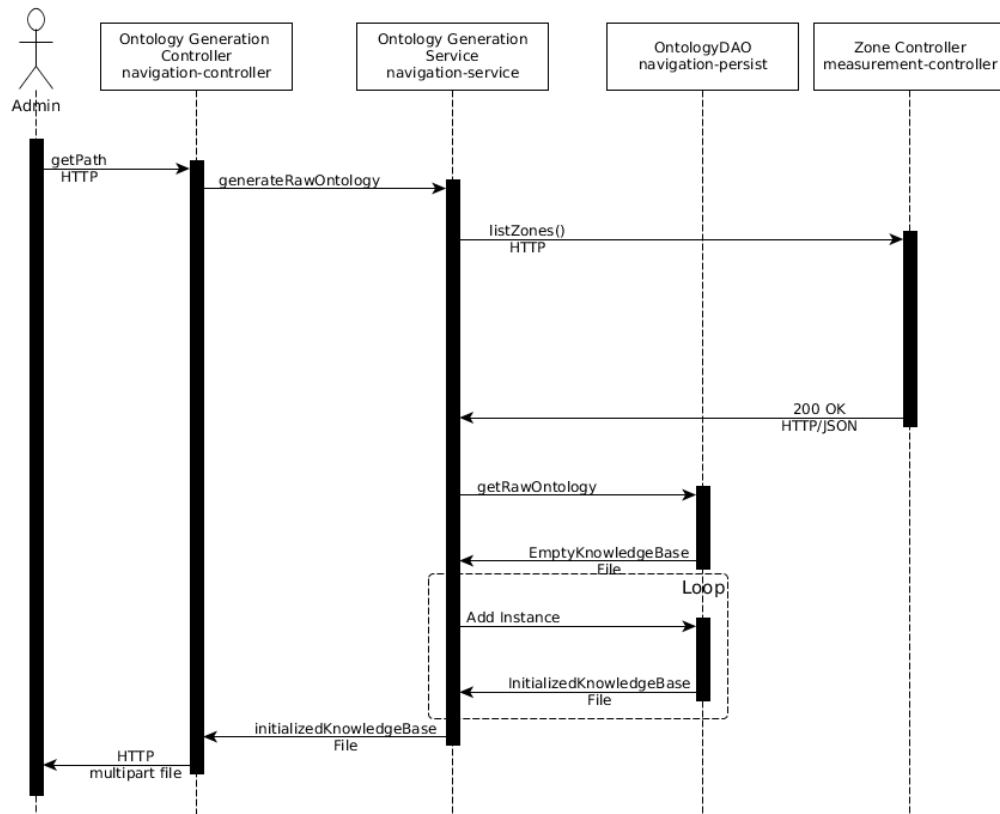


Fig. 5: Sequence diagram of the ontology generation process

the Business Logic is represented by the Service Tier and the Data Access Tier is denoted by the Persistence Tier.

The Web Tier provides an interface to the services provided and integrates the other modules of the navigation subsystem. Controllers are the entry points of the functions. The Data Transfer Objects are responsible for the conversion of domain objects into JSON format and simplify the HTTP messages. The application-context defines the configuration of the web application and it is used by the Spring Framework which is responsible for dependency injection.

The Service Tier contains the definition of service interfaces and their implementation. The ontology generation and way finding algorithms are implemented in this tier. The web controllers use these services via their interface so the concrete implementation can be changed. Hence, the extension of the ILONA System with other way finding algorithms would require only two steps. Firstly, the novel algorithm should be enclosed into a class that implements the interface of the way finding service. Then, the application should be reconfigured to use the way finding algorithm recently added.

The Persistence Tier is responsible for the storage and retrieval of domain objects. The measurement-persist and navigation-persist components are distinguished according to which subsystem they belong to. The measurement subsystem already implements functions to manage Measurement, Zone and Position objects that are the basic concepts of the ILONA System. The measurement subsystem stores the objects in a MySQL database that is separate from the navigation subsystem. The

navigation-persist component contains the ILONA ontology and provides methods for querying. The separation of the behavior and the implementation of storage facilitates the development and maintenance of the source code.

B. Test Results

The navigation subsystem was tested automatically and case studies were performed for demonstrating its usability. Unit tests are used to verify the behavior of the software components. In addition, they facilitate the developers' work and can be considered as a helpful complementary documentation. Based on de facto industrial standards, a component is well tested if at least 80% of the source code is covered. Finally, unit testing allows the evaluation of the component separately.

The automated tests covered the model, persist-ontology, service-impl and controller modules that contains the implementation. Table II shows the code coverage of the tests. The model and controller modules were entirely covered by the tests. The code coverage of the persist-ontology and the service-impl modules exceeded 96%, so it also satisfies the common industrial requirement that is around 80%. Although the automated tests cannot prove the validity of the implementation, they can detect failures. Due to the high code coverage, the validity of the implementation is accepted.

C. Experimental Results

The navigation subsystem was tested manually with real life scenarios in order to check its functionality. The tests were performed

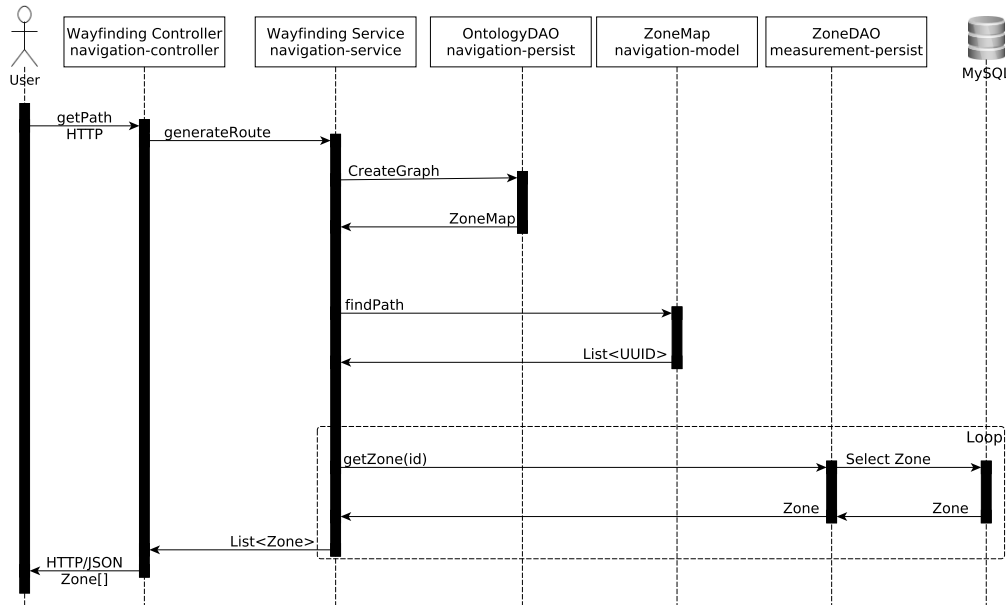


Fig. 6: Sequence diagram of the way finding process

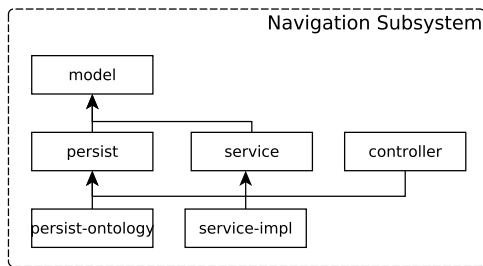


Fig. 7: Modules of the navigation subsystem

TABLE II: Code coverage of the navigation subsystem

Module	Coverage (%)
model	100
persist-ontology	97.8
service-impl	96.2
controller	100

in a three-story educational building that has both stairs and an elevator. Two case studies present the route between the entrance and Lecture Hall 205. The destination is located on the second floor in the rear of the building. The two scenarios are distinguished by the use and unuse of restrictions. During the way finding process the goal was to minimize zone transitions. Experimental results confirm the applicability of the navigation subsystem in real life scenarios.

Figure 9 shows the JSON messages that are sent between the server and the client during the experiments. Figure 9a shows the client request with the source and destination zones and with the given restriction. In Figure 9b we can see the server response with the suggested route, that is the list of zones leading from the start to the destination zone. The difference between the two cases is highlighted with italic text. As can be seen in Figure 9a, the `restriction` attribute of the request object is an empty array in the first case

while it contains the `no_elevator` string in the second case. When the restriction is set, the response object contains the `1st Floor Lobby` zone object too.

Without restrictions the system generated a route that used the elevator in the hall. First, the route leads from `Ground Floor Lobby` to `2nd Floor Lobby`. Then, the user shall go through `2nd Floor West Corridor` where the door of `Lecture Hall 205` is placed.

In the case when the `no_elevator` restriction was given, the generated route led through the stairs without the use of the elevator. So in the response, there is an additional zone whose name is `1st Floor Lobby`. These results meet with our expectations and fit the shortest path in the building whose floor plan can be checked in Figure 10.

IV. DISCUSSION

Extension of the ILONA System with an ontology-based indoor way finding function was presented in this paper. The extension allows zone level route generation that can facilitate the navigation within indoor environments. In addition, the presented way finding algorithm is integrated to the navigation subsystem of the ILONA System that is an open source indoor positioning and navigation framework. Thus, the presented method can be the base of indoor navigation solutions.

The ontology was designed to match the data model of the ILONA System and it is capable of modeling an indoor environment. The ontology defines five different kinds of gateways that allow the modeling of the connections between the zones. Distinguishing the gateways is necessary for disabled people who may want to avoid certain types of gateways. ILONA Ontology is used to create the knowledge base that represents the structure of buildings. The application of ontology reasoners facilitates the performing of complex queries and allows the extraction of various views of the indoor environment. The queried model was used to convert the task of way finding into finding the shortest path in a graph.

The ILONA System was used to implement the way finding algorithm. The implementation was added to the navigation subsystem that is broken down to components based on their functionality.

Ontology based Indoor Navigation Service for the ILONA System

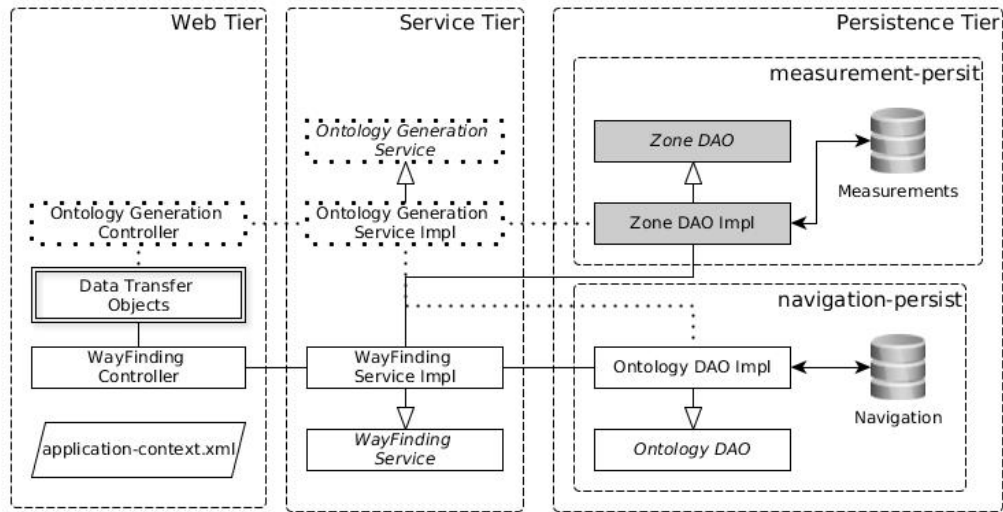


Fig. 8: Components used by the navigation service

```
{ "sourceID " : "25f79341-7256-4871-a2d5-2008ef88fd8e",
  "destID " : "fa162e02-b404-48c7-bc02-8469dbb1e052",
  "startName " : "Ground Floor Lobby",
  "destinationName " : "Lecture Hall 205",
  "restriction " : ["no_elevator"] }
```

(a) Request body

```
[{ "id " : "25f79341-7256-4871-a2d5-2008ef88fd8e",
  "name " : "Ground Floor Lobby" },
  { "id " : "d93e647e-4d17-4c3b-9d4c-dd8b88e4523c",
  "name " : "1st Floor Lobby" },
  { "id " : "d93e647e-4d17-4c3b-9d4c-dd8b88e4523c",
  "name " : "2nd Floor Lobby" },
  { "id " : "4adae318-49b6-42fb-a6a5-0eb2f0efd2f8",
  "name " : "2nd Floor West Corridor" },
  { "id " : "fa162e02-b404-48c7-bc02-8469dbb1e052",
  "name " : "Lecture Hall 205" } ]
```

(b) Response body

Fig. 9: JSON messages during the experiment

Both automatic and manual tests were used against the components and the navigation subsystem. Due to the high code coverage of the tests, the implementation of the way finding algorithm can be considered as verified. The experiments were performed in a three story building and the goal was to generate a route between the entrance and a room placed in the rear of the building. Routes were generated with and without restrictions and the yielded results matched our expectations. Hence, experimental results confirm the applicability of the way finding algorithm.

The presented ontology-based indoor way finding algorithm can be used as a reference in the ILONA System during the development of novel methods. Future investigations should focus on the time complexity of the way finding method, and the modeling of bigger environments in order to examine the limits of the presented way finding algorithm.

ACKNOWLEDGEMENTS

The described article was carried out as part of the EFOP-3.6.1-16-2016-00011 “Younger and Renewing University – Innovative Knowl-

edge City – institutional development of the University of Miskolc aiming at intelligent specialisation” project implemented in the framework of the Szechenyi 2020 program. The realization of this project is supported by the European Union, co-financed by the European Social Fund.

This research was supported by the European Union and the Hungarian State, co-financed by the European Regional Development Fund in the framework of the GINOP-2.3.4-15-2016-00004 project, aimed to promote the cooperation between higher education and industry.

REFERENCES

- [1] Christos Anagnostopoulos, Vassileios Tsetsos, Panayotis Kikiras, et al. Ontonav: A semantic indoor navigation system. In *1st Workshop on Semantics in Mobile Environments (SME05), Ayia*. Citeseer, 2005.
- [2] Patrick M Dudas, Mahsa Ghafourian, and Hassan A Karimi. Onalin: Ontology and algorithm for indoor routing. In *2009 Tenth International Conference on Mobile Data Management: Systems, Services and Middleware*, pages 720–725. IEEE, 2009.
- [3] Erich Gamma. *Design patterns: elements of reusable object-oriented software*. Pearson Education India, 1995.
- [4] Tom Gruber, In Ling Liu Ontology, and M Tamer Özsu. Encyclopedia of database systems. *Ontology*, 2009.
- [5] Dominik Heckmann, Tim Schwartz, Boris Brandherm, Michael Schmitz, and Margeritta von Wilamowitz-Moellendorff. Gumo—the general user model ontology. In *International Conference on User Modeling*, pages 428–432. Springer, 2005.
- [6] Matthew Horridge and Sean Bechhofer. The owl api: A java api for owl ontologies. *Semantic Web*, 2(1):11–21, 2011.
- [7] K. Ilku and J. Tamas. Indoorgml modeling: A case study. In *2018 19th International Carpathian Control Conference (ICCC)*, pages 633–638, May 2018.
- [8] Daniel P Kun, Erika Baksane Varga, and Zsolt Toth. Ontology based navigation model of the ilona system. In *Applied Machine Intelligence and Informatics (SAMII), 2017 IEEE 15th International Symposium on*, pages 479–484. IEEE, 2017.
- [9] Steffen Lohmann, Stefan Negru, Florian Haag, and Thomas Ertl. Vowl 2: user-oriented visualization of ontologies. In *International Conference on Knowledge Engineering and Knowledge Management*, pages 266–281. Springer, 2014.
- [10] Boris Motik, Peter F Patel-Schneider, Bijan Parsia, Conrad Bock, Achille Fokoue, Peter Haase, Rinke Hoekstra, Ian Horrocks, Alan Ruttenberg, Uli Sattler, et al. Owl 2 web ontology language: Structural specification and functional-style syntax. *W3C recommendation*, 27(65):159, 2009.

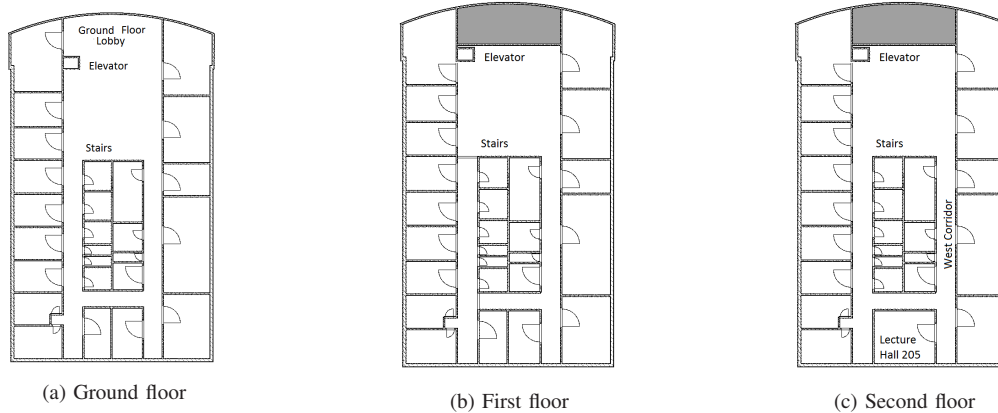


Fig. 10: Building floor plans

[11] Boris Motik, Rob Shearer, and Ian Horrocks. Hypertableau Reasoning for Description Logics. *Journal of Artificial Intelligence Research*, 36:165–228, 2009.

[12] Mark A Musen. The protégé project: A look back and a look forward. *AI matters*, 1(4):4–12, 2015.

[13] A. Satan. Bluetooth-based indoor navigation mobile system. In *2018 19th International Carpathian Control Conference (ICCC)*, pages 332–337, May 2018.

[14] Graeme Turnbull Stevenson, Juan Ye, Simon Andrew Dobson, and Paddy Nixon. Loc8: a location model and extensible framework for programming with location. *IEEE Pervasive Computing*, 2010.

[15] Zsolt Tóth, Péter Magnucz, Richárd Németh, and Judit Tamás. Data model for hybrid indoor positioning systems. *PRODUCTION SYSTEMS AND INFORMATION ENGINEERING*, 7:67–80, 2015.

[16] Zsolt Tóth. Ilona: indoor localization and navigation system. *Journal of Location Based Services*, 10(4):285–302, 2016.

[17] Xin Wang, Jianga Shang, Fangwen Yu, and Jinjin Yan. Indoor semantic location models for location-based services. *Int. J. Smart Home*, 7(4):127–136, 2013.

[18] Lei Yu, Yang Lu, and XiaoJuan Zhu. Smart hospital based on internet of things. *Journal of Networks*, 7(10):1654–1661, 2012.



Zsolt Tóth is a Lecturer in the Institute of Information Sciences at the University of Miskolc. He is also a member of the IEEE Computer Society. He received his PhD in Computer Science from the University of Miskolc. His research interests include indoor positioning and navigation techniques, applications of data mining, neural network, software development, web development and distributed systems. He has designed and supervises the development of the ILONA System and leads a research group focused on indoor positioning and navigation. He has over 30 publications.



Dániel Péter Kun has a Bachelor’s Degree in Business Informatics and a Master’s Degree in Software Engineering specialized in Application Development. For two years, he had been working on the ILONA System as a developer. His contribution to the navigation module of the ILONA System was valuable.



Erika Baksáné Varga is an associate professor at the Department of Information Technology in the University of Miskolc. She has MSc in Information Technology and Engineering Economics. Her research areas: ontology, natural language processing, data modeling, management and analysis, data- and knowledge intensive systems. Title of her PhD dissertation: Ontologybased semantic annotation and knowledge representation in a grammar induction system (2011).

Automatic classification possibilities of the voices of children with dysphonia

Miklós Gábor Tulics and Klára Vicsi

Abstract—Dysphonia is a common complaint, almost every fourth child produces a pathological voice. A mobile based filtering system, that can be used by pre-school workers in order to recognize dysphonic voiced children in order to get professional help as soon as possible, would be desired. The goal of this research is to identify acoustic parameters that are able to distinguish healthy voices of children from those with dysphonia voices of children. In addition, the possibility of automatic classification is examined. Two sample T-tests were used for statistical significance testing for the mean values of the acoustic parameters between healthy voices and those with dysphonia. A two-class classification was performed between the two groups using leave-one-out cross validation, with support vector machine (SVM) classifier. Formant frequencies, mel-frequency cepstral coefficients (MFCCs), Harmonics-to-Noise Ratio (HNR), Soft Phonation Index (SPI) and frequency band energy ratios, based on intrinsic mode functions ($IMF_{entropy}$) measured on different variations of phonemes showed statistical difference between the groups. A high classification accuracy of 93% was achieved by SVM with linear and rbf kernel using only 8 acoustic parameters. Additional data is needed to build a more general model, but this research can be a reference point in the classification of voices using continuous speech between healthy children and children with dysphonia.

Index Terms — voice disorder, statistical analysis, acoustic parameters, dysphonia, classification

I. INTRODUCTION

Dysphonia is a common complaint, reported in nearly one-third of the population at some point in their life. It affects the formation of clear and distinct sounds in speech as a complex function, a pathological condition showing various symptoms due to several etiologic factors and pathogenesis diversity [1]. The term dysphonia is often incorrectly used when referring to hoarseness, however hoarseness is a symptom of altered voice quality reported in patients, while dysphonia can be defined as altered pitch, loudness, or vocal quality or effort that impairs communication as assessed by a clinician and affects the patients' life [2]. The development of cheap, easy-to-use and lightweight methods that alert subjects of possible health problems is desired.

Mobile technology is attractive, since it is easy to use and it is a nearly constant feature of daily life. The number of mobile applications is growing in healthcare. A smartphone or tablet could be an ideal mobile tool to use with complex methods that

M. G. Tulics and K. Vicsi are with the Department of Telecommunications and Media Informatics, Budapest University of Technology and Economics, Magyar Tudósok krt. 2., Budapest 1117, Hungary
(email: tulics,vicsi@tmit.bme.hu., url: <http://www.tmit.bme.hu>)

can offer clues for general physicians in identifying the early stages of dysphonia.

Researchers target such applications for the early diagnosis of pathological voices in case of adults. In the work of [3] a mobile health (m-Health) application is presented for voice screening of adults by using a mobile device. The system is able to distinguish healthy voices from pathological ones using a noise-aware method that provides a robust estimation of the fundamental frequency during a sustained production of the vowel /a/.

Some systems record more than voice disorders, also recording other details regarding the general health of a patient. In [4] a healthcare framework based on the Internet of Things (IoT) and cloud computing, the system is able to capture voice, body temperature, electrocardiogram, and ambient humidity.

Most of the research on the subject currently focuses on the accurate estimation of dysphonia, rather than the development of practical applications.

Dysphonia affects patients of all ages, however research suggests that risks are higher in pediatric and elderly (>65 years of age) populations. 23.4% of pediatric patients have dysphonia at some point during their childhood [5], [6], [7], [8]. The data therefore suggests that almost every fourth child produces a pathological voice. Studies agree that dysphonia is more often reported among boys than girls, the ratio being 70-30%.

In the last 10-20 years many studies focused on dysphonia in adults, not only on sustained vowels, but on running speech as well [9], [10]. However, in the literature we can find some studies focusing on the dysphonic voices of children.

Previous studies regarding the analysis of pathological children's voice focused mainly on sustained vowels. Researchers mostly work with small sample sizes because it is difficult to collect recordings from children. Janete Coelho and his colleagues [11] analyzed the perceptual and acoustic vocal parameters of school age children with vocal nodules and to compared them with a group of children without vocal nodules. Five children were examined from both genders, aged from 7 to 12 years. The Mann-Whitney U test, with $p < 0.05$ significance level was used in their work. Statistically significant differences were registered between the group of vocal nodules vs. the group without vocal nodules, on the following parameters: fundamental frequency, shimmer, HNR, maximum phonation time for /a/ e /z/, s/z coefficient and GRBASI (Grade, Roughness, Breathiness, Asthenia, Strain, Instability). On jitter and maximum phonation time for /s/ there were no statistically significant differences.

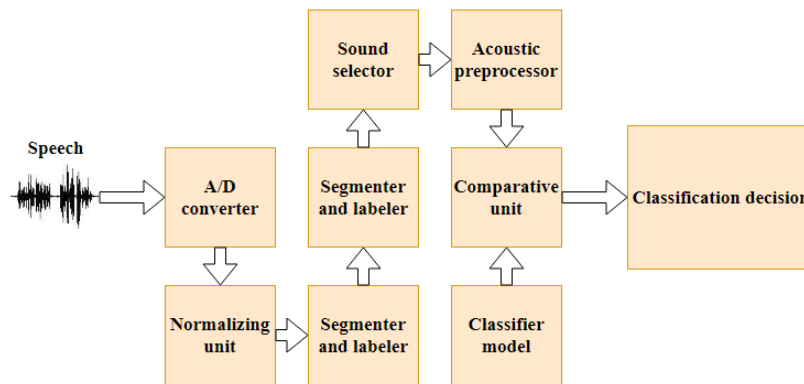


Fig. 1. Proposed framework for the recognition of dysphonic voiced children

The study of Gopi Kishore Pebbili and his colleagues [12] aimed to document the Dysphonia Severity Index (DSI) scores of 42 Indian children aged 8–12 years. DSI values were found to be significantly higher ($p=0.027$) in girls than in boys. DSI attempts to measure the severity of dysphonia based on the sustained production of a vowel, using a weighted combination of maximum phonation time, highest frequency, lowest intensity, and jitter (%) of an individual.

In [13] correlation between perceptual and acoustic data was examined to identify measures that are useful in determining the severity of voice deviation in children. Recordings from 71 children (aged 3–9 years) were used, containing the sustained sound /ε/ and the counting of numbers from 1 to 10. Results showed that F0 measures correlate with strain to phonate; shimmer and GNE parameters correlate with general degree of voice deviation.

In our earlier research [14] continuous speech was examined, where we investigated the relationship between the voices of healthy children and those with functional dysphonia (FD). The statistical analyses drew the conclusion that variations of jitter and shimmer values with HNR (Harmonics-to-Noise Ratio) and the first component (c1) of the mel-frequency cepstral coefficients (referred to as ‘MFCC01’) are good indicators to separate healthy voices from voices with FD in the case of children. Samples from healthy children and adult voices were also compared giving a clear conclusion that differences exist in the examined acoustical parameters even between the two groups. It is necessary to carry out the investigations separately on children’s voices as well; we cannot use adult voices to draw any conclusions regarding children’s voices.

The goal of this research is to identify further acoustic parameters that are able to distinguish healthy voices of children from ones with dysphonia. For this reason statistical analyses was prepared, followed by a detailed classification experiment. Thus, setting a basis of a future mobile health application for the early recognition of dysphonia in the case of children.

Section 2 briefly describes the speech material used in the experiments, followed by the description of the measured acoustic parameters, the statistical evaluation, parameter

reduction and model building. Our results are shown in Section 3, followed by the discussion and the future direction in Section 4.

II. MATERIALS AND METHODS

A diagnostic support system for the early recognition of dysphonia in the voices of children would follow the logic described in Fig 1. The A/D converter digitizes the analogue speech signal of the child, after which the signal is normalized. In continuous speech, the measuring locations must be determined. Since in this work the acoustic parameters are measured on phonemes, phoneme level segmentation is required. Acoustic parameters (described in paragraph B) are extracted from the selected phonemes and arranged into a feature vector. The feature vector is given to a classifier to perform binary classification (healthy or unhealthy). Prior knowledge is gained by the processing of a carefully built speech database (described in paragraph A) and an optimal classification model using the acoustic parameters with great distinguishing power (classifier model). The system produces an output; this decision is shown on the user interface of the application. This study focuses on the automatic classification of voices of children with dysphonia.

A. Dysphonic and Healthy Child Speech Database

Sound samples from children were collected at several kindergartens. All the recordings were made with parental consent, mostly in the presence of the children’s parents. The children recited a poem entitled “The Squirrel”, written by a logopedic specialist. This poem was chosen for therapeutic reasons, speech therapists using the poem during treatment, and because children in the 5-10 year old age group are very fond of the poem and it is easy for them to learn. The most frequent vowel in the poem is the vowel [o], with 16 pieces followed by 14 pieces of the vowel [O] and 9 pieces of vowel [E].

The recordings were made using a near field microphone (Monacor ECM-100), Creative Soundblaster Audigy 2 NX outer USB sound card, with 44.100 Hz sampling rate and 16-bit linear coding. The duration of the recordings is about 20 seconds each.

All recordings were annotated and segmented on phoneme level, using the SAMPA phonetic alphabet [15]. In the rest of this article, vowels and other sounds will be referred with SAMPA characters in brackets. The segmentation was made with the help of an automatic phoneme segmentator, which was developed in our laboratory, followed by manual corrections. A total of 59 recordings were used in this work: 25 voices from children with dysphonia (mean age: 6.52(±1.94)) (3 children had vocal nodes, the rest had functional dysphonia) and 34 recordings from healthy children (mean age: 5.35(±0.54)). Table I summarizes the recordings from the database used in the experiments.

B. Acoustic parameters

In our earlier study [14], statistical analyses draw the conclusion that acoustic parameters like jitter, shimmer, HNR and the first component (c1) of the mel-frequency cepstral coefficients are good indicators to separate healthy and dysphonic voices in case of children. These acoustic parameters showed significant difference on vowels [E], [o], [O], [A:]. Since the most frequent vowel in the poem is the [o], it is sufficient to extract these acoustic parameters on it.

In this work, we are attempting to expand the set of used acoustic parameters that could be helpful in the automatic classification of children with healthy voices from those with dysphonic ones.

In our earlier work [16] we demonstrated Soft Phonation Index (SPI) and Empirical mode decomposition (EMD) based frequency band ratios (IMF_{entropy}) acoustic parameters measured on different phonetic classes (for example nasals, vowels, fricatives etc.) correlate with the severity of dysphonia in adult speech. Further parameters also needs to be investigated in continuous children speech.

The following acoustic parameters were used in this study: **Fundamental frequency (F0)** means, standard deviations and ranges were calculated on vowels [E] and [o]. The fundamental frequency calculation was done by an autocorrelation method described in [17].

Formant frequency (F1, F2, F3) means, standard deviations and ranges were calculated on vowels [E] and [o].

Formant frequency bandwidth (F1BW, F2BW, F3BW) means, standard deviations and ranges were calculated on vowels [E] and [o]. Formant frequency tracking was realized by applying Gaussian window for a 150 ms long signal at a 10 ms rate. For each frame LPC coefficients were measured. The algorithm can be found in [16]. In case of fundamental frequency and formant frequencies we wanted to examine if there is a difference between the vowel [E] and [o]. Vowel [E] was used by us in adult speech.

Jitter(ddp), shimmer(ddp), HNR (Harmonics-to-Noise Ratio) means, standard deviations and ranges were calculated on vowel [o]. Jitter is the average absolute difference between consecutive time periods (T) in speech, divided by the average time period. Calculation of jitter goes as follows:

$$jitter(ddp) = \frac{\sum_{i=2}^{N-1} |2 \cdot T_i - T_{i-1} - T_{i+1}|}{\sum_{i=2}^{N-1} T_i} * 100 [\%] \tag{1}$$

where N is the number of periods, and T is the length of the periods. Shimmer is the average absolute difference between consecutive differences between the amplitudes of consecutive periods. Its calculation goes in a similar way:

$$shimmer(ddp) = \frac{\sum_{i=2}^{N-1} |2 \cdot A_i - A_{i-1} - A_{i+1}|}{\sum_{i=2}^{N-1} A_i} * 100 [\%] \tag{2}$$

HNR represents the degree of acoustic periodicity. It is calculated with the following formula:

$$HNR = 10 * \log \frac{E_H}{E_N} [dB] \tag{3}$$

where E_H is the energy of the harmonic component, while E_N is the energy of the noise component.

12 MFCC (mel-frequency cepstral coefficients) means, standard deviations and ranges were calculated on vowel [o]. MFCCs are widely used in automatic speech and speaker recognition, where frequency bands are equally spaced on the mel scale, that approximates the human auditory system's response. To calculate the MFCCs one needs to do the following steps: first we need to frame the signal into short frames, for each frame we need to calculate the periodogram estimate of the power spectrum. Then apply the mel filterbank to the power spectra, sum the energy in each filter and take the logarithm of all filterbank energies. MFCCs are the output of a Discrete Cosine Transform (DCT) on spectral values P_j . DCT is given by the following equation:

$$c_{k-1} = \sum_{j=1}^N P_j \cos\left(\frac{\pi(k-1)}{N}(j-0,5)\right) \tag{4}$$

where N represents the number of spectral values and P_j the power in dB of the jth spectral value (k runs from 1 to N).

SPI (Soft Phonation Index) and **IMF_{entropy}** means, standard deviations and ranges were calculated on vowel [o], nasals ([m], [n] and [J]), low vowels, high vowels, voiced spirants ([v], [z] and [Z]), voiced plosives and affricates ([b], [d], [g], [dz], [dZ] and [d']). Moreover, SPI was calculated on the whole sample as well. SPI is the average ratio of energy of the speech signal in the low frequency band (70-1600 Hz) to the high frequency band (1600-4500 Hz). If the ratio is large that means the energy is concentrated in the low frequencies, indicating a softer voice [17].

IMF_{entropy} is an empirical mode decomposition (EMD) based frequency band ratio acoustic parameter. EMD decomposes a multicomponent signal into elementary signal components called intrinsic mode functions (IMFs) [20]. Each of these IMFs contributes both in amplitude and frequency towards generating the speech signal. The IMFs are arranged in a matrix in sorted order according to frequency. The first few IMFs are the high frequency components of the signal, the latter IMFs represent the lower frequency components. We calculate the entropy (E) for each IMF. The frequency band ratios of entropy were calculated the following way:

$$IMF_{entropy} = \frac{\sum_{d=1}^2 E_d}{\sum_{d=2}^D E_d} \tag{5}$$

H_d is the value of Shannon entropy for each $d = 1, 2, \dots, D$ of the log-transformed IMFs. D is the total number of extracted IMFs, while the Shannon entropy for a discrete signal is defined as

$$E(p_i) = -K \sum_{i=1}^n p_i \log p_i \tag{6}$$

where K is a positive constant.

Thus, in this research 124 acoustic parameters were calculated (acoustic parameter set using all 124 parameters further referred to as “starting parameters”). For the extraction of the acoustic parameters a software was used that was developed in the Laboratory of Speech Acoustics.

C. Statistical analyses of acoustic parameters and decision methods

T-test compares two averages (means) and concludes if they are different from each other. It also shows us how significant the differences are. In other words, it lets us know if those differences could have happened by chance. Two sample T-tests were used for statistical significance testing for the mean values of the acoustic parameters between healthy voices and those with dysphonia (all parameters obtained were disposed by using SPSS20.0 software). Where F tests showed significant variances of an acoustic parameter within the groups (with significance level 95% ($\alpha = 0.05$), Welch’s T-test was used. Welch’s T-test is insensitive to equality of the variances regardless of whether the sample sizes are similar. Our assumption is that the distributions are normal, but T tests are relatively robust to moderate violations of the normality assumption.

D. Feature selection and classification

A two-class classification was performed between healthy children and children suffering from dysphonia using leave-one-out cross validation, with SVM (support vector machine) classifier. SVM is a supervised machine-learning algorithm that is used mainly for binary classification tasks (for machine-learning tests, RapidMiner Studio 7.5 was used). SVM was used in this research because the classifier has achieved good results in the classification of healthy and pathological speech in the case of adults.

While with the help of the T-test we can identify all the acoustic parameters that are significantly different in the examined two groups one-by-one, it does not give us all the acoustic parameters that are useful in the automatic classification. Significant parameters may have high correlations with each other and this examination does not say anything about possible useful parameter combinations. Subsets that are more effective for classification may exist, instead of selecting only significant parameters. In the hope of finding the best acoustic parameter subset as input vector Forward feature selection algorithm was used. This is an iterative algorithm, which chooses the best feature that improves the accuracy in regards of a cost or objective function (maximum accuracy), in each step by adding an acoustic

TABLE I
THE CHILD VOICE DATABASE USED

<i>Diagnosis</i>			
<i>Sex</i>	<i>Dysphonia</i>	<i>Healthy</i>	<i>Sum</i>
<i>Girl</i>	5	15	20
<i>Boy</i>	20	19	39
<i>Sum</i>	25	34	59

parameter to the set of parameters already chosen. It starts with an empty set and stops after a number (here with set this number to 3) of generations without improval. In this way, the FFS algorithm also reduces dimensionality.

III. RESULTS

A. Statistical analysis of healthy voices and voices of children suffering from dysphonia

In the statistical analysis, the null hypothesis states that the means of the two groups are equal. The calculated p-value is a probability that measures the evidence against the null hypothesis. A smaller p-value provides stronger evidence against the null hypothesis. To determine whether the difference between the two group means is statistically significant we compare the p-value to a significance level. In practice, 0.1, 0.05 and 0.01 significance levels are used. The significance level of 0.05 represents a 5% risk and concludes that there is a difference when there is no real difference.

F0, jitter(ddp) and shimmer(ddp) means, standard deviations and ranges did not show significant difference between the two groups.

Formant frequencies, MFCCs, HNR, SPI and IMF_{entropy} showed significant difference in more cases, presented in Table II. The table shows summary statistics for acoustic parameters significant at 0.1 significance level. Formant frequencies were significant in case of vowel [o], but not in case of [E]. This can be explained with the difference in the number of occurrences of the vowels.

B. Classification results

In the binary classification experiment, several cases were examined, trying out different input vectors. For classification an SVM classifier was used with linear and radial basis function (rbf) kernel. Each parameter is scaled to [0, 1].

First, all the parameters calculated were used as input. Acoustic parameters which showed significant difference with at least $p < 0.1$ significance level were selected separately and used as input vector as well. Note that if an acoustic parameter does not show significant difference between the voices of healthy children and the voices of ones with dysphonia it can still have great distinguishing power. For this reason, the Forward feature selection (FFS) algorithm was used.

Automatic classification possibilities of the voices of children with dysphonia

TABLE II
ACOUSTIC PARAMETERS SIGNIFICANT AT 0.1 LEVEL.

Acoustic parameter	Group	Mean	Std. Deviation	p-value	Acoustic parameter	Group	Mean	Std. Deviation	p-value
F2.mean_[o]	Healthy	1162.925	184.223	0.085	MFCC.std_[o]_9	Healthy	8.488	1.006	0.000
	Dysphonia	1086.651	133.979			Dysphonia	10.096	1.274	
F2.std_[o]	Healthy	265.705	73.338	0.082	MFCC.range_[o]_9	Healthy	48.096	6.023	0.012
	Dysphonia	233.993	60.123			Dysphonia	53.218	9.103	
F2.range_[o]	Healthy	956.021	263.749	0.061	HNR.mean_[o]	Healthy	11.010	2.113	0.081
	Dysphonia	833.932	208.948			Dysphonia	10.039	2.024	
F2BW.mean_[o]	Healthy	299.412	94.392	0.078	HNR.std_[o]	Healthy	2.522	1.081	0.026
	Dysphonia	262.145	50.294			Dysphonia	3.259	1.394	
F3BW.mean_[o]	Healthy	763.094	244.427	0.018	HNR.range_[o]	Healthy	8.926	3.496	0.049
	Dysphonia	606.681	243.545			Dysphonia	10.799	3.578	
F3BW.range_[o]	Healthy	1264.323	290.436	0.085	SPI.raw	Healthy	0.942	0.108	0.060
	Dysphonia	1099.791	429.988			Dysphonia	1.003	0.134	
MFCC.mean_[o]_1	Healthy	277.215	16.839	0.025	SPI.mean_[o]	Healthy	1.515	0.190	0.048
	Dysphonia	289.069	22.780			Dysphonia	1.611	0.163	
MFCC.std_[o]_1	Healthy	19.432	2.988	0.056	SPI.std_[o]	Healthy	0.295	0.044	0.006
	Dysphonia	22.158	6.380			Dysphonia	0.340	0.067	
MFCC.range_[o]_1	Healthy	98.992	16.438	0.005	SPI.range_[o]	Healthy	1.391	0.232	0.002
	Dysphonia	114.361	24.042			Dysphonia	1.604	0.258	
MFCC.range_[o]_2	Healthy	93.164	17.010	0.040	SPI.range_[m-n-J]	Healthy	1.359	0.248	0.035
	Dysphonia	103.124	19.280			Dysphonia	1.495	0.227	
MFCC.range_[o]_3	Healthy	92.916	13.919	0.058	SPI.mean_[O-A:-o-u]	Healthy	1.321	0.164	0.069
	Dysphonia	100.211	14.896			Dysphonia	1.396	0.140	
MFCC.std_[o]_4	Healthy	15.072	2.618	0.001	SPI.std_[O-A:-o-u]	Healthy	0.380	0.062	0.002
	Dysphonia	17.304	2.185			Dysphonia	0.432	0.059	
MFCC.range_[o]_4	Healthy	76.543	14.040	0.001	SPI.range_[O-A:-o-u]	Healthy	1.868	0.386	0.017
	Dysphonia	88.539	10.948			Dysphonia	2.063	0.215	
MFCC.std_[o]_5	Healthy	12.461	1.801	0.031	SPI.mean_[v-z-Z]	Healthy	0.908	0.240	0.031
	Dysphonia	13.712	2.550			Dysphonia	1.059	0.285	
MFCC.range_[o]_5	Healthy	66.465	9.360	0.024	SPI.mean_[b-d-g-dz-dZ-d']	Healthy	1.148	0.273	0.071
	Dysphonia	74.682	15.462			Dysphonia	1.271	0.227	
MFCC.mean_[o]_6	Healthy	-13.625	6.726	0.003	IMF_ENTROPY.std_[o]	Healthy	0.234	0.056	0.091
	Dysphonia	-8.662	5.205			Dysphonia	0.208	0.059	
MFCC.range_[o]_6	Healthy	59.224	7.114	0.035	IMF_ENTROPY.range_[o]	Healthy	0.886	0.252	0.017
	Dysphonia	65.273	12.366			Dysphonia	0.736	0.203	
MFCC.std_[o]_7	Healthy	10.604	1.856	0.053	IMF_ENTROPY.mean_[m-n-J]	Healthy	1.290	0.294	0.082
	Dysphonia	11.657	2.233			Dysphonia	1.148	0.318	
MFCC.mean_[o]_8	Healthy	-7.773	4.003	0.079					
	Dysphonia	-9.634	3.877						

TABLE III
TWO-CLASS CLASSIFICATION RESULTS.

Case number	Acoustic parameters	Number of parameters	Kernel	Hyper-parameters	Accuracy (%)
1	Starting parameters	124	linear	C=1	88.13%
2	Starting parameters	124	rbf	C= 124; gamma= 0.008	86.44%
3	Significant parameters (p<0.1)	37	linear	C=1	72.88%
4	Significant parameters (p<0.1)	37	rbf	C= 37; gamma= 0.027	69.49%
5	FFS with linear kernel	8	linear	C=1	93.22%
6	FFS with rbf kernel	8	rbf	C=10; gamma=0.1	93.22%

In this experiment, in the case of rbf kernel the hyperparameter C is set to the number of parameters, while gamma is set to 1/number of parameters. When using FSS we cannot know how many parameters will be chosen by the algorithm, the hyper-parameters are chosen by intuition. Leave-one-out cross validation was used in all cases. Classification results are summarized in Table III.

As Table III shows that the highest accuracy of 93% was reached using linear and rbf kernel. The features selection algorithm reduced the input dimensionality to 8 acoustic parameters, while achieving higher accuracy than the case when the starting parameters were used. The acoustic parameters selected by the FFS algorithm in case of linear kernel are the following: F3.range_[o], MFCC.range_[o]_3, MFCC.range_[o]_4, MFCC.mean_[o]_5, MFCC.range_[o]_8, MFCC.std_[o]_9, MFCC.mean_[o]_11, HNR.mean_[o].

When using rbf kernel the parameter selection algorithm also selected 8 parameters, namely: F2.range_[o], MFCC.mean_[o]_4, MFCC.std_[o]_9, MFCC.std_[o]_10, MFCC.mean_[o]_12, SHIMMER.range_[o], SPI.std_[O-A:-o-u], SPI.range_[v-z-Z]. This combination also achieved 93% accuracy.

We can conclude that these parameter combinations have great power to distinguish healthy from dysphonic voices of children.

IV. DISCUSSION AND CONCLUSIONS

The present study investigated the relationship between healthy and dysphonic voices of children using continuous speech. The classification results are good; in the long term it is worth developing a tool for the automatic detection of dysphonic voices among children. Mobile devices are suitable for implementing this method and using it in practice.

Mobile health applications are usually designed for smartphones or tablets, on some occasions smartwatches. They allow users to access information when and where they need it; reducing time wasted searching for specific data. These devices are cheap, easy-to-use and lightweight. Voice samples, metadata, acoustic parameter values and the classifier output

can be collected and uploaded to a cloud server. In this way, we can monitor the quality of the children's voice over the long term.

A. Database

It was essential to create a well-structured speech database containing children's speech samples, both from healthy children and children suffering from dysphonia. The database used in this research contains 59 recordings: 25 voices from children with dysphonia and 34 healthy children. Three children from the dysphonic group had vocal nodes, the rest had functional dysphonia.

Earlier research confirmed that is necessary to carry out the investigations separately on children's voices as well, we cannot use adult voices to make any conclusions to children's voices.

B. Statistical analysis

Through statistical analyses we drew the conclusion that formant frequencies, MFCCs, HNR, SPI and $IMF_{entropy}$ measured on different variations of phonemes are good indicators to separate healthy and dysphonic voices in the case of children. F0, jitter and shimmer means, standard deviations and ranges did not show significant difference between the two groups.

C. Two-class classification and parameter selection

During classification experiments, a high classification accuracy of 93% was reached using SVM with linear and rbf kernel and reducing dimensionality to 8 acoustic parameters. It is worth mentioning that selecting only the acoustic parameters that showed significant difference did not improve the classification accuracy.

Due to small sample size overfitting might be problem. This occurs when a model begins to "memorize" the detail and noise in the training data, rather than "learning", to generalize from a trend. Although overfitting happens more often with nonparametric nonlinear models, our highest accuracy was reached with a linear model as well. We cannot conclude that the problem is solved; much more data is needed to obtain better and more general results.

Automatic classification possibilities of the voices of children with dysphonia

The trend however is clear and promising; the automatic separation of healthy from pathological voices in the case of children is possible. This research can be a reference point in the classification of the voices of healthy children and voices of children with dysphonia using continuous speech.

D. Future work

The goal is to build a filtering system that can be used by pre-school workers. If a child with dysphonic voice can be filtered in time, they have a better chance of getting a professional help from an ear, nose and throat (ENT) specialist or a speech therapist.

Future work includes collecting further speech records to generalize the classification model on a larger dataset. There are possibilities to optimize the model as well, for example by tuning the hyper-parameters of an estimator with grid-search. The automatic annotation and segmentation of the speech recordings implemented in a smartphone-based system, and the automatic assessment of the severity of dysphonia is also desirable. We also believe that the results are generalizable to other languages.

V. ACKNOWLEDGEMENT

We would like to thank Mária Ágostházy from the Speech Therapy and Vocational Education Service of Újbuda and Beke-Nádas Éva from the Cseresznyevirág Art Kindergarten for helping us construct the Dysphonic and Healthy Child Speech Database.

REFERENCES

[1] Hirschberg J., Hacki T. és Mészáros K. (szerk.), "Foniátria és társtudományok: A hangképzés, a beszéd és a nyelv, a hallás és a nyelés élettana, kórtana, diagnosztikája és terápiája (I. kötet)". Budapest: *Eötvös Kiadó*. 2013.

[2] Stachler, Robert J., et al. "Clinical Practice Guideline: Hoarseness (Dysphonia)(Update) Executive Summary." *Otolaryngology-Head and Neck Surgery* 158.3 (2018): 409-426.

[3] Verde, Laura, et al. "An m-health system for the estimation of voice disorders." *Multimedia & Expo Workshops (ICMEW)*, 2015 IEEE International Conference on. IEEE, 2015.

[4] Muhammad, Ghulam, et al. "Smart health solution integrating IoT and cloud: a case study of voice pathology monitoring." *IEEE Communications Magazine* 55.1, 2017: 69-73.

[5] Bhattacharya N. "The prevalence of pediatric voice and swallowing problems in the United States", *Laryngoscope*, 2015;125:746-750.

[6] Duff MC, Proctor A, Yairi E., "Prevalence of voice disorders in African American and European American preschoolers", *J Voice*, 2004;18:348-353.

[7] Carding PN, Roulstone S, Northstone K, et al., "The prevalence of childhood dysphonia: a cross-sectional study", *J Voice*, 2006;20:623-630.

[8] Silverman EM, "Incidence of chronic hoarseness among schoolage children", *J Speech Hear Disord*. 1975;40:211-215.

[9] Kazinczi, F., Mészáros, K., Vicsi, K., "Automatic detection of voice disorders", in: *International Conference on Statistical Language and Speech Processing*, Springer. pp. 143–152, 2015.

[10] Grygiel, J., StrumoHo, P., Niebudek-Bogusz, E., "Application of mel cepstral representation of voice recordings for diagnosing vocal disorders", *Delta* 12, 2, 2012.

[11] Coelho, Janete, et al. "Vocal nodules in school age children." *Revista de Logopedia, Foniatria y Audiologia* 36.3 (2016): 103-108.

[12] Pebbili, Gopi Kishore, Jui Kidwai, and Srushti Shabnam. "Dysphonia Severity Index in typically developing Indian children." *Journal of Voice* 31.1, 2017: 125-e1.

[13] Lopes, Leonardo Wanderley, et al. "Severity of voice disorders in children: correlations between perceptual and acoustic data." *Journal of Voice* 26.6, 2012: 819-e7.

[14] Tulics, Miklós Gábor, Ferenc Kazinczi, and Klára Vicsi. "Statistical analysis of acoustical parameters in the voice of children with juvenile dysphonia." *International Conference on Speech and Computer*. Springer, Cham, 2016.

[15] Klára, Vicsi: „SAMPA computer readable phonetic alphabet, Hungarian,” 2008.

[16] Tulics, Miklós Gábor, and Klára, Vicsi. "Phonetic-class based correlation analysis for severity of dysphonia." *Cognitive Infocommunications (CogInfoCom)*, 2017 8th IEEE International Conference on. IEEE, 2017.

[17] Paul Boersma. "Accurate short-term analysis of the fundamental frequency and the harmonics-to-noise ratio of a sampled sound", *Proceedings of the Institute of Phonetic Sciences* 17, 1193, pp. 97- 110.

[18] Press, William H., et al. "Numerical Recipes in C: The Art of Scientific Computing (10.5) Cambridge University Press." *Cambridge*, 1992.

[19] Roussel, N.C., Lobdell, M., "The clinical utility of the soft phonation index", *Clinical linguistics & phonetics* 20, 181–186, 2006.

[20] Huang, N.E., Shen, Z., Long, S.R., Wu, M.C., Shih, H.H., Zheng, Q., Yen, N.C., Tung, C.C., Liu, H.H., "The empirical mode decomposition and the hilbert spectrum for nonlinear and non-stationary time series analysis", in: *Proceedings of the Royal Society of London A: mathematical, physical and engineering sciences*, The Royal Society. pp. 903–995, 1998.



Miklós Gábor Tulics was born in Baia Mare, Romania, on Aug. 15, 1988. He is currently a technical assistant and a Ph.D. candidate at the Laboratory of Speech Acoustics, Budapest University of Technology and Economics, focusing on automatic speech recognition, machine learning and pathological voice disorder recognition. He earned his Master’s degree in Electrical Engineering in 2015. Tulics has been working part time for the Department of Telecommunications and Media Informatics, Budapest University of Technology and Economics since 2013.



Klára Vicsi DSc Ph.D. is currently a lead research professor and was the Chief of the Laboratory of Speech Acoustics of the Department of Telecommunications and Media Informatics at Budapest University of Technology and Economics from 2002 until 2018. She earned her Master’s degree at the Loránd Eötvös University of Sciences, Budapest in 1966-1971. She earned her DSc degree at the Hungarian Academy of Sciences in 2005, her PhD degree at the Technical University of Budapest in 1992, and her Doctor’s degree at Loránd Eötvös University of Sciences in 1982. She has worked as a researcher and lecturer, participated in conferences and congresses in several countries such as Germany, California USA, Finland and Poland. She is responsible for the organization of many international conferences, workshops and summer schools. She holds project manager and participant member status in several international research projects such as: Contact person, of CLARIN, FLAReNet, ELSNET. She is the leader of the Acoustical Complex Committee of the Hungarian Academy of Sciences, a Member of ISCA and a member of the scientific board of journals. She has more than 122 publications in peer-reviewed journals, 67 refereed conference proceedings and is the owner of three patents.



The 4th IEEE/IFIP International Workshop on Analytics for Network and Service Management (AnNet 2019) will be held in conjunction with the IFIP/IEEE International Symposium on Integrated Network Management (IM) in Washington DC, USA on April 8, 2019.

Following the success of its previous editions, AnNet aims to present research and experience results in data analytics and machine learning for network and service management. Approaches such as statistical analysis, data mining and machine learning are promising to harness the immense stream of operational data and to improve operations and management of IT systems and networks.

AnNet 2019 will include original full-paper presentations, a keynote, and short-paper sessions. The workshop attendees will be stimulated to participate in interesting discussions. Short papers describing late-breaking advances and work-in-progress reports from ongoing research and experimental work are also welcome.

TOPICS OF INTEREST

Authors are invited to submit papers that fall into or are related to one or multiple topic areas listed below:

Data Analytics

- Analysis, modeling and visualization
- Operational analytics and intelligence
- Event, log and big data analytics
- Network traffic analysis
- Anomaly detection and prediction
- Crowd sensing
- Monitoring and measurements for management
- Predictive and real-time analytics
- Harnessing social data for management

Machine Learning Techniques

- Supervised, semi-supervised, and unsupervised learning
- Clustering and data mining
- Reinforcement learning
- Multi-agent based learning
- Deep learning
- Bayesian methods
- Ensemble methods
- Cognitive computing
- Mining spatiotemporal and time series data

Network Management Paradigms

- Autonomous and autonomic networks
- Fog/edge computing
- In-network processing
- Bio-inspired networks and self-management
- Cognitive and software defined networks
- Network function virtualization
- Security, fault, performance, and resource management

Application Domains

- Computer networks
- Mobile ad-hoc and wireless sensor networks
- Clouds and data centers
- Virtualized infrastructures
- Internet of Things
- Computing and network services
- IT service management, storage resource management

PAPER SUBMISSION

Paper submissions must present original, unpublished research or experiences. Only original papers that have not been published or submitted for publication elsewhere can be submitted. Each submission must be written in English, accompanied by a 75 to 200 words abstract that clearly outlines the scope and contributions of the paper. There is a length limitation of 6 pages (including title, abstract, all figures, tables, and references) for regular papers, and 4 pages for short papers describing work in progress. Submissions must be in IEEE 2-column style. Self-plagiarized papers will be rejected without further review. Authors should submit their papers via JEMS:

https://submissoes.sbc.org.br/im2019_anNet

PROCEEDINGS

Papers accepted for AnNet 2019 will be included in the conference proceedings, IEEE Xplore, IFIP database and EI Index. IFIP and IEEE reserve the right to remove any paper from the IFIP database and IEEE Xplore if the paper is not presented by one of its authors at the workshop. Awards will be presented to the best paper at the workshop.

GENERAL CHAIR

- Nur Zincir-Heywood, Dalhousie University, Canada

TPC CO-CHAIRS

- Idilio Drago, Politecnico di Torino, Italy
- Robert Harper, Moogsoft, UK

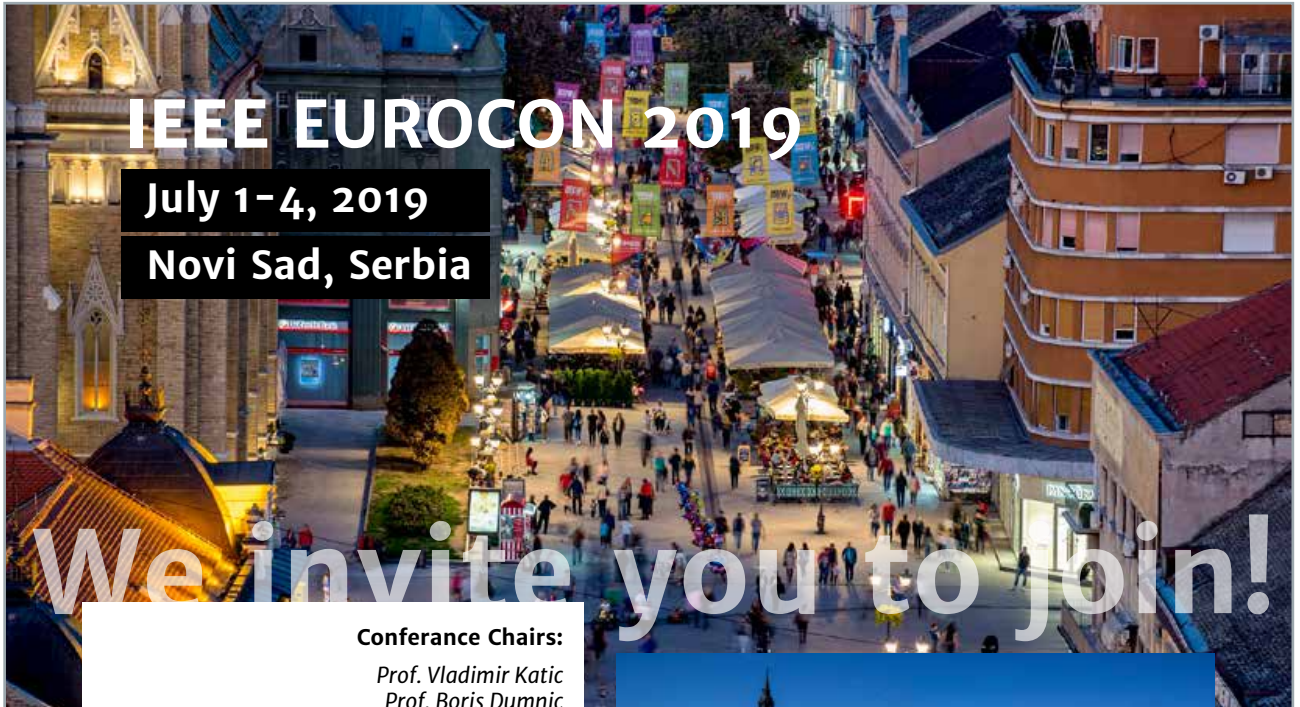
STEERING COMMITTEE

- Raouf Boutaba, University of Waterloo, Canada
- Yixin Diao, IBM T. J. Watson Research Center, USA
- Rolf Stadler, KTH Royal Institute of Technology, Sweden
- Filip De Turck, Ghent University – iMinds, Belgium
- Mehmet Ulema, Manhattan College, USA
- Nur Zincir-Heywood, Dalhousie University, Canada

IMPORTANT DATES

- Paper Registration: **November 16, 2018**
- Paper Submission Deadline: **November 20, 2018**
- Acceptance Notification: **December 20, 2018**
- Camera-Ready Papers: **January 15, 2019**
- Workshop Date: **April 8, 2019**

For more information, see: <http://annet2019.moogsoft.com/>



Conference Chairs:

Prof. Vladimir Katic
Prof. Boris Dumnic
 University of Novi Sad
 Faculty of Technical Sciences

Technical Program Chair:

Prof. Marko Delimar
 University of Zagreb
 Faculty of Electrical Engineering and
 Computing

Publication Chair:

Prof. Cedomir Stefanovic
 Aalborg University Copenhagen
 The Technical Faculty of IT and Design
 Department of Electronic Systems

EUROCON

is a flagship event of the IEEE Region 8 (Europe, Middle East and Africa) held every two years in a different country with participants from all over the world.

EUROCON is a major international forum for the exchange of ideas, theory basics, design methodologies, techniques and experimental results between academia, research institutions and practitioners from industry. It has achieved a considerable success during the past 16 editions in all fields of electrical and electronic engineering, ICT and computer science covered by IEEE Societies



Images provided by: Tourist Organisation of the City of Novi Sad

The magnificent city of Novi Sad is the second largest city in Serbia and the capital of autonomous province of Vojvodina. City's natural landscape and the numerous galleries, museums and monasteries make it one of the most popular destinations in region. The city lies on the Danube river, which splits Petrovaradin fortress and the city center. Petrovaradin fortress, as a city's art center, is a place which mysterious underground keeps intriguing explorers from around the world, due to its rich history. Novi Sad is elected as European Youth Capital for 2019, as well as European Capital of Culture for 2021 for its large cultural and creative potential. As one of the leading educational and research centers in Central Europe, the University of Novi Sad is home to more than 50,000 students and 5,000 employees. With beautiful harmony of nature and modern architecture, the central University building will be the venue where main conference activities are held. Novi Sad is also home to 18 year old music festival EXIT, the winner of 'Best Major European festival' award (more information: <https://www.exitfest.org/en>). Bring your highest spirit with you, because EXIT begins immediately after the conference!

[web page: eurocon2019.org](http://eurocon2019.org)

Important dates

Full paper submission / **November 23, 2018**
 Paper acceptance notification / **February 04, 2019**
 Camera-ready papers and early registration / **April 06, 2019**
 Special Session proposals deadline / **November 30, 2018**

The technical sessions:

Track 1: Information, Communication and Technology;
Track 2: Circuits, Systems and Signal Processing;
Track 3: Power Engineering and Energy;
Track 4: Industry and Consumer Applications.

KEYNOTE LECTURES:



Trends in acquisition and monitoring of human physiological parameters
 Dr. Voicu Groza, P.Eng., Fellow IEEE, Fellow EIC
 Professor and Associate Director, Computer Engineering
 School of Electrical Engineering and Computer Science,
 University of Ottawa, CANADA



How Reliability, Latency, Massiveness, and Blockchain are Transforming IoT Communication
 Petar Popovski, Ph. D., FIEEE
 Professor in Wireless Communications
 Head of the Section on Connectivity
 Department of Electronic Systems
 Aalborg University, Denmark



Flexibility in power system management for enhanced reliability
 Dirk Van Hertem
 Associate Professor KU Leuven
 Department of electrical engineering (ESAT)
 Katholieke Universiteit Leuven, Belgium

CONFERENCE TOPICS:

Aerospace and Electronic Systems; Antennas and Propagation; Broadcast Technology; Circuits and Systems; Communications; Components, Packaging, and Manufacturing Technology; Computational Intelligence; Computer Engineering; Consumer Electronics; Control Systems; Dielectrics and Electrical Insulation; Education; Electron Devices; Electromagnetic Compatibility; Engineering in Medicine and Biology; Geoscience and Remote Sensing; Industrial Electronics; Industry Applications; Information Theory; Instrumentation and Measurement; Intelligent Transportation Systems; Magnetics; Mechatronics; Microwave Theory and Techniques; Nano- and Micro-Electronics; Nuclear and Plasma; Oceanic Engineering; Photonics; Power Electronics; Power & Energy; Product Safety Engineering; Professional Communication; Reliability; Robotics and Automation; Signal and Image Processing; Social Implications of Technology; Solid-State Circuits; Systems, Man, and Cybernetics; Technology & Engineering Management; Ultrasonics, Ferroelectrics, & Frequency Control; Vehicular Technology.

IEEE R8 Student Paper Contest SPC 2019 awards will be presented at the conference.
<https://ieeer8.org/student-activities/>

The conference includes a student competition and the **EUROCON 2019 Best Student Paper Award**.

Contact

Conference Secretariat – Eurocon 2019
 University of Novi Sad
 Faculty of Technical Sciences
 Trg Dositeja Obradovica 6
 21000 Novi Sad, Serbia
 Phone: **+381 21 450-810**
 Fax: **+381 21 458 133**
 Email: **secretariat@eurocon2019.org**
 Web: **eurocon2019.org**

Sponsors



Serbia and Montenegro Section

Under auspices of



MINISTRY OF EDUCATION, SCIENCE AND TECHNOLOGICAL DEVELOPMENT, REPUBLIC OF SERBIA, BELGRADE



PROVINCIAL SECRETARIAT FOR HIGHER EDUCATION AND SCIENTIFIC RESEARCH ACTIVITY, AP VOJVODINA, NOVI SAD

Guidelines for our Authors

Format of the manuscripts

Original manuscripts and final versions of papers should be submitted in IEEE format according to the formatting instructions available on

http://www.ieee.org/publications_standards/publications/authors/authors_journals.html#sect2,

“Template and Instructions on How to Create Your Paper”.

Length of the manuscripts

The length of papers in the aforementioned format should be 6-8 journal pages.

Wherever appropriate, include 1-2 figures or tables per journal page.

Paper structure

Papers should follow the standard structure, consisting of *Introduction* (the part of paper numbered by “1”), and *Conclusion* (the last numbered part) and several *Sections* in between.

The Introduction should introduce the topic, tell why the subject of the paper is important, summarize the state of the art with references to existing works and underline the main innovative results of the paper. The Introduction should conclude with outlining the structure of the paper.

Accompanying parts

Papers should be accompanied by an *Abstract* and a few *index terms (Keywords)*. For the final version of accepted papers, please send the *short cvs* and *photos* of the authors as well.

Authors

In the title of the paper, authors are listed in the order given in the submitted manuscript. Their full affiliations and e-mail addresses will be given in a footnote on the first page as shown in the template. No degrees or other titles of the authors are given. Memberships of IEEE, HTE and other professional societies will be indicated so please supply this information. When submitting the manuscript, one of the authors should be indicated as corresponding author providing his/her postal address, fax number and telephone number for eventual correspondence and communication with the Editorial Board.

References

References should be listed at the end of the paper in the IEEE format, see below:

- a) Last name of author or authors and first name or initials, or name of organization
- b) Title of article in quotation marks
- c) Title of periodical in full and set in italics
- d) Volume, number, and, if available, part
- e) First and last pages of article
- f) Date of issue

[11] Boggs, S.A. and Fujimoto, N., “Techniques and instrumentation for measurement of transients in gas-insulated switchgear,” *IEEE Transactions on Electrical Installation*, vol. ET-19, no. 2, pp.87–92, April 1984.

Format of a book reference:

[26] Peck, R.B., Hanson, W.E., and Thornburn, T.H., *Foundation Engineering*, 2nd ed. New York: McGraw-Hill, 1972, pp.230–292.

All references should be referred by the corresponding numbers in the text.

Figures

Figures should be black-and-white, clear, and drawn by the authors. Do not use figures or pictures downloaded from the Internet. Figures and pictures should be submitted also as separate files. Captions are obligatory. Within the text, references should be made by figure numbers, e.g. “see Fig. 2.”

When using figures from other printed materials, exact references and note on copyright should be included. Obtaining the copyright is the responsibility of authors.

Contact address

Authors are requested to submit their papers electronically via the EasyChair system. The link for submission can be found on the journal’s website: www.infocommunications.hu/for-our-authors

If you have any question about the journal or the submission process, please do not hesitate to contact us via e-mail:

Rolland Vida – Editor-in-Chief:
vida@tmit.bme.hu

Pál Varga – Associate Editor-in-Chief:
pvarga@hit.bme.hu



IEEE Global Communications Conference

9-13 December 2019 • Big Island, Hawaii, USA

Revolutionizing Communications

CALL FOR PAPERS AND PROPOSALS

The 2019 IEEE Global Communications Conference (GLOBECOM) will be held in Waikoloa on the beautiful Big Island, Hawaii, USA, from **9-13 December 2019**. Themed "*Revolutionizing Communications*," this flagship conference of the IEEE Communications Society will feature a comprehensive high-quality technical program including 13 symposia and a variety of tutorials and workshops. IEEE GLOBECOM 2019 will also include an attractive Industry program aimed at practitioners, with keynotes and panels from prominent research, industry and government leaders, business and industry panels, and vendor exhibits.

IMPORTANT DATES

Paper Submission 15 April 2019 (23:59)	Tutorial Proposals 15 March 2019
Acceptance Notification 15 July 2019	Workshop Proposals 15 Feb 2019
Camera-Ready 16 August 2019	Industry Proposals 1 June 2019

Full details of submission procedures are available at globecom2019.ieee-globecom.org

TECHNICAL SYMPOSIA

- Ad Hoc and Sensor Networks
 - Cognitive Radio and Networks
 - Communication and Information Systems Security
 - Communication QoS, Reliability and Modeling
 - Communication Software, Services & Multimedia Apps.
 - Communication Theory
 - Green Communication Systems and Networks
 - Next-Generation Networking and Internet
 - Optical Networks & Systems
 - Signal Processing for Communications
 - Wireless Communications
 - Mobile & Wireless Networks
- Selected Areas in Communications
 - Access Networks/Systems & Power Line Communications
 - Big Data
 - Cloud & Fog/Edge Computing, Networking and Storage
 - E-Health
 - Internet of Things
 - Molecular, Biological and Multi-Scale Communications
 - Satellite and Space Communications
 - Smart Grid Communications
 - Social Networks
 - Tactile Internet

INDUSTRY FORUMS AND EXHIBITION PROGRAM

Proposals are sought for forums, panels, demos, seminars and presentations specifically related to issues facing the broader communications and networking industries.

TUTORIALS

Proposals are invited for half- or full-day tutorials in all communication and networking topics.

WORKSHOPS

Proposals are invited for half- or full-day workshops in all communication and networking topics.

ORGANIZING COMMITTEE

Honorary Chair

Vint Cerf, Google, USA

General Chair

Doug Zuckerman, Vencore Labs, USA

Vice General Chair

Thomas Moore, Troptel (Retired)

Technical Program Chair

Hsiao-Hwa Chen, NCKU, Taiwan

Technical Program Vice Chairs

Hamid Gharavi, NIST, USA
Chonggang Wang, InterDigital Commun, USA

Technical Panels Chairs

Russell Hsing, NCTU, Taiwan
Ying-Dar Lin, NCTU, Taiwan

Tutorials Chairs

Venkatesha Prasad, TUDelft, Netherlands
Albena Mihovska, Aarhus University, Denmark

Workshops Chairs

Yi Qian, U. of Nebraska-Lincoln, USA
Li-Chun Wang, NCTU, Taiwan

Industry Forums & Exhibition Chair

Mehmet Ulema, Manhattan College, USA

Operations Chair

James W-K Hong, Postech, Korea

globecom2019.ieee-globecom.org

SCIENTIFIC ASSOCIATION FOR INFOCOMMUNICATIONS



Who we are

Founded in 1949, the Scientific Association for Infocommunications (formerly known as Scientific Society for Telecommunications) is a voluntary and autonomous professional society of engineers and economists, researchers and businessmen, managers and educational, regulatory and other professionals working in the fields of telecommunications, broadcasting, electronics, information and media technologies in Hungary.

Besides its 1000 individual members, the Scientific Association for Infocommunications (in Hungarian: HÍRKÖZLÉSI ÉS INFORMATIKAI TUDOMÁNYOS EGYESÜLET, HTE) has more than 60 corporate members as well. Among them there are large companies and small-and-medium enterprises with industrial, trade, service-providing, research and development activities, as well as educational institutions and research centers.

HTE is a Sister Society of the Institute of Electrical and Electronics Engineers, Inc. (IEEE) and the IEEE Communications Society.

What we do

HTE has a broad range of activities that aim to promote the convergence of information and communication technologies and the deployment of synergic applications and services, to broaden the knowledge and skills of our members, to facilitate the exchange of ideas and experiences, as well as to integrate and

harmonize the professional opinions and standpoints derived from various group interests and market dynamics.

To achieve these goals, we...

- contribute to the analysis of technical, economic, and social questions related to our field of competence, and forward the synthesized opinion of our experts to scientific, legislative, industrial and educational organizations and institutions;
- follow the national and international trends and results related to our field of competence, foster the professional and business relations between foreign and Hungarian companies and institutes;
- organize an extensive range of lectures, seminars, debates, conferences, exhibitions, company presentations, and club events in order to transfer and deploy scientific, technical and economic knowledge and skills;
- promote professional secondary and higher education and take active part in the development of professional education, teaching and training;
- establish and maintain relations with other domestic and foreign fellow associations, IEEE sister societies;
- award prizes for outstanding scientific, educational, managerial, commercial and/or societal activities and achievements in the fields of infocommunication.

Contact information

President: **GÁBOR MAGYAR, PhD** • elnok@hte.hu

Secretary-General: **ERZSÉBET BÁNKUTI** • bankutie@ahrt.hu

Operations Director: **PÉTER NAGY** • nagy.peter@hte.hu

International Affairs: **ROLLAND VIDA, PhD** • vida@tmit.bme.hu

Address: H-1051 Budapest, Bajcsy-Zsilinszky str. 12, HUNGARY, Room: 502

Phone: +36 1 353 1027

E-mail: info@hte.hu, Web: www.hte.hu